Role of Criegee intermediates in the formation of sulfuric acid at a Mediterranean (Cape Corsica) site under influence of biogenic emissions

Alexandre Kukui[1], Michel Chartier[1], Jinhe Wang[2,3], Hui Chen[3,a], Sébastien Dusanter[4], Stéphane Sauvage[4], Vincent Michoud[4,b], Nadine Locoge[4], Valérie Gros[5], Thierry Bourrianne[6], Karine Sellegri[7], Jean-Marc Pichon[7]

[1] Laboratoire de Physique et Chimie de l'Environnement et de l'Espace (LPC2E), CNRS Orléans, France
[2] Resources and Environment Innovation Research Institute, School of Municipal and Environmental Engineering, Shandong Jianzhu University, Jinan 250101, China
[3] ICARE-CNRS, 1 C Av. de la Recherche Scientifique, 45071 Orléans CEDEX 2, France
[4] IMT Lille Douai, Institut Mines -Télécom, Univ. Lille, Centre for Energy and Environment, F-59000 Lille, France
[5] Laboratoire des Sciences du Climat et de l'Environnement (LSCE), UMR CNRS-CEA-UVSQ, IPSL, Univ. Paris-Saclay, F-91191 Gif Sur Yvette, France
[6] Centre National de Recherches Météorologiques (CNRM), GMEI, MNP, Météo-France, F-31057 Toulouse, France
[7] Laboratoire de Météorologie Physique Observatoire de Physique du Globe (LAMP), Clermont-Ferrand, France
[a] now in Shanghai Key Laboratory of Atmospheric Particle Pollution and Prevention, Department of Environmental Science and Engineering, Institute of Atmospheric Sciences, Fudan University, Shanghai 200438, China
[b] now in Université de Paris, Université Paris Est Créteil (UPEC), UMR CNRS 7583, Laboratoire Interuniversitaire des Systèmes Atmosphériques, Paris, France

Correspondence to: Alexandre Kukui (alexandre.kukui@cnrs-orleans.fr)

Abstract. Reaction of stabilized Criegee Intermediates (SCIs) with SO_2 was proposed as an additional pathway of gaseous sulfuric acid (H_2SO_4) formation in the atmosphere, supplementary to the conventional mechanism of H_2SO_4 production by oxidation of SO_2 in reaction with OH radicals. However, because of a large uncertainty in mechanism and rate coefficients for the atmospheric formation and loss reactions of different SCIs, the importance of this additional source is not well established. In this work, we present an estimation of the role of SCIs in H_2SO_4 formation at a western Mediterranean (Cape Corsica) remote site, where a comprehensive field observations including gas phase H_2SO_4, OH radicals, SO_2, volatile organic compounds (VOCs) and aerosol size distribution measurements have been performed in July - August 2013 as a part of the project ChArMEx. The measurement site was under strong influence of local emissions of biogenic volatile organic compounds including monoterpenes and isoprene generating SCIs in reactions with ozone and, hence, presenting an additional source of H_2SO_4 via SO_2 oxidation by the SCIs. Assuming the validity of a steady state between H_2SO_4 production and its loss by condensation on existing aerosol particles with a unity accommodation coefficient, about 90% of the H_2SO_4 formation during the day could be explained by the reaction of SO_2 with OH. During the night the oxidation of SO_2 by OH radicals was found to contribute only about 10% to the H_2SO_4 formation. The accuracy of the derived values for the contribution of $OH+SO_2$ reaction to the H_2SO_4 formation is limited mostly by a large, presently of a factor of 2, uncertainty in $OH+SO_2$ reaction rate coefficient. The contribution of the SO_2 oxidation by SCIs to the H_2SO_4 formation was evaluated using available measurements

of unsaturated VOCs and steady state SCIs concentrations estimated by adopting rate coefficients for SCIs reactions based on structure–activity relationships (SARs). The estimated concentration of the sum of SCIs was in the range of $(1 - 3) \times 10^3$ molecule cm^{-3}. During the day the reaction of SCIs with SO_2 was found to account for about 10% and during the night for about 40% of the H_2SO_4 production, closing the H_2SO_4 budget during the day but leaving unexplained about 50% of the H_2SO_4 formation during the night. Despite large uncertainties in used kinetic parameters, these results indicate that the SO_2 oxidation by SCIs may represent an important H_2SO_4 source in VOCs-rich environments, especially during night-time.

1 Introduction

Sulfuric acid, H_2SO_4, is an important atmospheric component identified to play a key role in formation of secondary atmospheric aerosol through new particles formation processes (Dunne et al., 2016; Paasonen et al., 2010; Sipilä et al., 2010; Weber et al., 1997). H_2SO_4 is considered as a major precursor of newly formed atmospheric nucleation-mode particles and may play a significant role in their subsequent growth (Boy et al., 2005; Smith et al., 2005; Zhang et al., 2012). It is therefore important to well understand the atmospheric mechanisms determining the H_2SO_4 concentrations in different atmospheric environments.

Until recently it was generally accepted that the dominant atmospheric source of H_2SO_4 is the reaction of OH radicals with SO_2 (R1) presenting a rate limiting step leading in the troposphere to a fast production of H_2SO_4 in presence of water vapour and oxygen via reactions (R2 - R3) (Finlayson-Pitts and Pitts Jr, 2000). It was assumed that H_2SO_4 atmospheric concentrations are determined predominantly by this source and the loss of sulphuric acid on the surface of existing particles with the loss rate depending on the efficiency of H_2SO_4 uptake.

$$OH + SO_2 \rightarrow HSO_3 \qquad\qquad (R1)$$

$$HSO_3 + O_2 \rightarrow SO_3 + HO_2 \qquad\qquad (R2)$$

$$SO_3 + H_2O \ (+H_2O) \rightarrow H_2SO_4 + H_2O \qquad\qquad (R3)$$
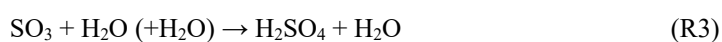
Another possible atmospheric source of H_2SO_4 via oxidation of SO_2 by stabilized Criegee intermediates (SCIs), compounds formed by ozonolysis of unsaturated organic compounds, was suggested by Cox and Penkett (1971) and discussed first in view of its atmospheric importance by Calvert and Stockwell (1983). For a long time the reactions of SO_2 with SCIs were considered as being too slow to represent an important atmospheric source of H_2SO_4, until in the more recent study of Welz et al. (2012) a rate constant of $(3.9\pm0.7)\times10^{-11}$ cm^{-3} molecule^{-1} s^{-1} was derived for the reaction of SO_2 with the simplest SCI, formaldehyde oxide (CH_2OO), which is significantly larger than previous estimates of around 4×10^{-15} cm^{-3} molecule^{-1} s^{-1} for the reactions of SO_2 with CH_2OO (Hatakeyama et al., 1986) and for the reactions of SO_2 with other SCIs (Johnson and Marston, 2008). The importance of this additional source of H_2SO_4 which is still under discussion depends on the atmospheric SCIs concentrations and the kinetics and mechanisms of the SCIs reactions with SO_2.

Criegee intermediates (CIs), also known as carbonyl oxides $(R_1)(R_2)COO$ with R_1 and R_2 representing different substituents, are produced via ozonolysis of alkenes by cycloaddition of an ozone molecule on a double bond forming a primary ozonide (POZ), a highly energized compound containing an O-O-O group. Subsequent rapid cleavage of either of the O-O bonds leads to the formation of a carbonyl compound and chemically activated CIs, which can undergo either prompt dissociation or thermal stabilization leading to the formation of the SCIs (Criegee, 1975; Criegee and Wenner, 1949; Donahue et al., 2011; Johnson and Marston, 2008; Vereecken and Francisco, 2012; Vereecken et al., 2012).

Atmospheric concentrations of SCIs depend on their production rates, by the ozonolysis of alkenes, and their loss rates, predominantly via unimolecular decomposition and reactions with water monomers and dimers (Vereecken et al., 2017). However, the kinetic parameters and the reaction mechanism of these processes are not well known.

The SCIs production rate is determined by the ozonolysis reaction rate constants and corresponding speciated yields of different SCIs. The speciated SCI yield depends on a relative yield of two different CIs formed by decomposition of the POZ and a yield of SCI produced by the CI collisional stabilization depending on the CI structure and its energy content. For most of atmospherically relevant alkenes, the total SCI yields were not studied directly, while for those for which multiple studies are available there is in many cases a large data scatter. The data on the speciated SCI yields are available only for a few of alkenes (see e.g. Vereecken et al. (2017) and references therein).

For the loss of SCIs via unimolecular decomposition and reactions with water monomers and dimers, the results of experimental and theoretical studies show that the corresponding rate coefficients may vary by orders of magnitude depending on the SCI substituents and conformers (see e.g. Vereecken et al. (2017) and references therein). In recent years experimental studies of these reactions with direct detection and generation of specific SCIs were performed for several among the simplest of them, such as formaldehyde oxide (CH_2OO) (Chao et al., 2015; Lewis et al., 2015; Sheps et al., 2017; Smith et al., 2015; Stone et al., 2018), acetaldehyde oxide (CH_3CHOO) (Li et al., 2020; Lin et al., 2016; Sheps et al., 2014) and acetone oxide (($CH_3)_2COO$) (Chhantyal-Pun et al., 2017; Fang et al., 2017; Huang et al., 2015; Lester and Klippenstein, 2018; Smith et al., 2016). Very recently the decomposition rate and an estimation of the rate coefficients for the reaction with water vapor were obtained for the first time in direct kinetic studies for *syn* Methyl Vinyl Ketone oxide (*syn*-MVK-oxide), and *anti* Methacrolein Oxide (*anti*-MACR-oxide), four-carbon unsaturated Criegee intermediates derived from the ozonolysis of isoprene (Barber et al., 2018; Caravan et al., 2020; Lin et al., 2021). For other large SCIs only estimations based on theoretical and indirect studies are available for their reactions with water vapor and their thermal decomposition.

The result of Welz et al. (2012) about the fast reaction of SO_2 with formaldehyde oxide was extended in later direct and indirect studies where similarly fast reactions with SO_2 were confirmed for CH_3CHOO, $(CH_3)_2COO$, Z-nopinone oxide (product of β-pinene ozonolysis), *syn*-MVK-oxide and *anti*-MACR-oxide (Ahrens et al., 2014; Caravan et al., 2020; Lin et al., 2021; Vereecken et al., 2017 and references therein), with rate coefficients in the range of $(3\text{-}16) \times 10^{-11}$ cm^3 $molecule^{-1}$ s^{-1}. Reactions of other SCIs with SO_2 were suggested to be similarly fast on the basis of theoretical results (Kurtén et al., 2011).

Theoretical analysis suggests that the reaction of SCI with SO_2 proceeds via a barrierless cycloaddition of SO_2 to SCI forming a sulfur-bearing secondary ozonide (SOZ) which can either be stabilized or decompose to form SO_3 or other products

(Kurtén et al., 2011; Kuwata et al., 2015; Vereecken et al., 2012). For smaller SCIs, e.g. formaldehyde and acetone oxides, the theory predicts negligible SOZ stabilization and about unity yield of SO_3 (Kuwata et al., 2015). These results are supported by experimental studies for CH_2OO (Berndt et al., 2014a; Wang et al., 2018) and $(CH_3)_2OO$, CH_3CHOO (Berndt et al., 2014b). For larger SCIs with expected longer SOZ lifetime the SO_3 yield may depend on the SOZ fate in the atmosphere with respect to its decomposition or further reactions, e.g. with H_2O, (Kuwata et al., 2015; Vereecken et al., 2012), although a large yield of sulfur trioxide exceeding 80% was observed by Ahrens et al. (2014) for the large SCI formed during the ozonolysis of β-pinene

Estimations based on the available or evaluated kinetic parameters show that the atmospheric SCI concentrations vary by orders of magnitude depending on conditions specific for different environments, such as the concentrations and composition of alkenes, ozone concentration or humidity. Using chemistry-transport global modeling the highest SCI concentrations of the order of $10^4 – 10^5$ molecule cm^{-3} were inferred for the regions with highest isoprene and terpenes emissions, e.g. above the tropical forest (Chhantyal-Pun et al., 2019; Khan et al., 2018; Newland et al., 2018; Vereecken et al., 2017; Novelli et al., 2017). Estimated using steady-state calculations, the concentration of SCI ranges from 2.3×10^3 molecule cm^{-3} at a rural site to 5.5×10^4 molecule cm^{-3} in an urban polluted environment (Vereecken et al., 2017). The estimated contribution of SCI to H_2SO_4 formation is also highly variable: about 7% in rural environments and up to 70% over tropical regions (Vereecken et al., 2017). At the global scale, the contribution of SCI to SO_2 oxidation was estimated to be negligible, contributing less than 1% (Newland et al., 2018). The uncertainty associated to the predicted SCI concentrations was estimated to be one order of magnitude (Vereecken et al., 2017), due to poorly defined SCI formation and loss rates. Even a higher uncertainty may be expected for the estimated contribution of SCIs to SO_2 oxidation considering not well defined reaction rate coefficients for the reaction of different SCIs with SO_2.

The adequacy of the mechanism treating the SO_2 oxidation by OH as a predominant source of the atmospheric H_2SO_4 was tested in a number of field campaigns where simultaneous measurements of OH and H_2SO_4 were conducted (Supplement, p. 2, Table S1). Selected ion Chemical Ionisation Mass Spectrometry (CIMS) technique for simultaneous measurements of OH and H_2SO_4 was first introduced by (Eisele and Tanner, 1993) and since then it has been used in a number of field measurements in different environments. In these studies the measurements of OH, H_2SO_4, SO_2 and aerosol surface area were used to compare the rate of H_2SO_4 production in reaction (R1) and the rate of H_2SO_4 loss on aerosol particles assuming steady state condition between these processes. In a number of measurements campaigns the H_2SO_4 budget was found to be closed using the uptake coefficient of unity corresponding to upper limit of the H_2SO_4 loss rate on existing particles. This was observed in different environments including remote marine (Weber et al., 1997), forested rural (Birmili et al., 2000; Boy et al., 2013) and forested remote sites (Eisele and Tanner, 1993; Weber et al., 1997). However, in other field studies conducted in various environments the H_2SO_4 condensation sink calculated using an uptake coefficient of unity was found to significantly exceed its formation rate via SO_2 oxidation by OH indicating either an H_2SO_4 uptake efficiency lower than unity or the presence of sources of H_2SO_4 other than reaction (R1) (Bardouki et al., 2003; Berresheim et al., 2002, 2014; Boy et al., 2013; Jefferson et al., 1998; Mauldin III et al., 2012; Petäjä et al., 2009). Several additional H_2SO_4 gas phase sources were suggested such as the oxidation

of DMS or DMDS in remote coastal environments proceeding with SO_3 formation (Berresheim et al., 2002, 2014; Jefferson et al., 1998) or SO_2 oxidation by SCIs in the boreal forest and in moderately polluted environments (Boy et al., 2013; Kim et al., 2015; Mauldin III et al., 2012). A heterogeneous formation of gas phase H_2SO_4 via the catalytic oxidation of SO_2 on the surface of black carbon aerosols has also been recently shown to be important under polluted conditions (Yao et al., 2020).

In this work, we present an evaluation of the role of SCIs in H_2SO_4 production at a remote site on Cape Corsica near the North tip of Corsica Island (Ersa station, western Mediterranean). In July - early August 2013, comprehensive field observations including gas phase (OH radicals, H_2SO_4, VOCs, NO_x, SO_2, others) and aerosol size distribution measurements were conducted at this site in the frame of the SAFMED (Secondary Aerosol Formation in the Mediterranean) campaign as part of the summer 2013 experimental effort of the project ChArMEx (the Chemistry-Aerosols Mediterranean Experiment). During the field campaign, the site was strongly influenced by local emissions of biogenic volatile organic compounds, including isoprene and terpenes, forming different SCIs in reactions with ozone and, hence, potentially representing an additional source of H_2SO_4 via reactions of SCIs with SO_2. We use the OH, H_2SO_4 and SO_2 measurements to estimate an upper limit for the contribution of H_2SO_4 sources other than reaction (R1). Using available measurements of unsaturated VOCs and adopting rate coefficients for SCIs reactions based on structure–activity relationships (SARs) from Vereecken et al. (2017), we estimate steady-state SCIs concentrations. These SCIs concentrations are used for the estimation of the rate of H_2SO_4 formation in the reactions of SCIs with SO_2 and its comparison with OH+SO_2 source resulting from the OH and H_2SO_4 measurements.

2 Methods

2.1 Field site

Measurements were performed at the Ersa site from 18 July to 5 August 2013 during ChArMEx/SAFFMED field campaign (Dulac et al., 2021). The Ersa station (42.969°N, 9.380°E) is located at Cape Corsica on the northern edge of Corsica (Michoud et al., 2017; Zannoni et al., 2017). It is situated at an altitude of 533 meters above sea level on the top of a hill dominating the northern part of the cape. On its eastern, northern and western sides it is a few km away from the coast and has a direct view of the sea. The measurement site is isolated by a mountain range from the closest large city, Bastia, situated about 30 km south of the site. The site is surrounded by widespread vegetation such as scrubland typical of the Mediterranean areas, responsible of biogenic VOC emissions (Debevec et al., 2021; Zannoni et al., 2015).

2.2 Experimental Methods

2.2.1 OH and H_2SO_4 measurements

Concentrations of OH radicals and H_2SO_4, as well as total peroxy radicals (HO_2+RO_2, not discussed here), were measured using chemical ionization mass spectrometry (CIMS) (Berresheim et al., 2000; Eisele and Tanner, 1991). A detailed description

of the instrument is presented elsewhere (Kukui et al., 2008, 2012). Here we briefly present the measurement technique and essential details about the setup and performance of the instrument during the ChArMEx/SAFMED campaign. A detailed description of the calibration system used during the campaign, which was not presented before, is given in Supplement, pp. 4-12, Sect. S3.

OH was detected by conversion of the sampled OH with isotopically labelled $^{34}SO_2$ to form $H_2^{34}SO_4$ in a chemical conversion reactor (CCR) in presence of ambient water vapour and oxygen. The isotopically labeled $H_2^{34}SO_4$ and ambient H_2SO_4 were detected by mass spectrometry as $H^{34}SO_4^-$ and $H^{32}SO_4^-$ product ions. The product ions were produced by chemical ionization with NO_3^- reagent ion in an ion-molecule reactor (IMR) following the CCR. The reagent ions were generated in a corona NO_2/air discharge ion source (CD). A scheme of the reactor is presented in Supplement, p. 5, Fig. S2.

Ambient air was sampled at a volumetric flow rate of 10 SLM (Standard Liter per Minute) creating turbulent flow in the chemical conversion region of the reactor. The turbulent flow conditions minimize possible influence of wind speed on the measurements and ensure fast mixing of reactants. The reactants used for the chemical conversion ($^{34}SO_2$ for OH conversion into sulfuric acid and NO for peroxy radicals conversion into OH and their subsequent detection as OH) and the radical quencher (NO_2) are introduced into the reactor through a set of injectors. NO_2 used as a scavenger removes not only the OH radicals, but also peroxy radicals converting them into HO_2NO_2 and RO_2NO_2 peroxy nitrates. Switching the reactant flows between the different injectors allows measurements in four different modes: the background mode, two different OH radical measurement modes and the peroxy radicals measurement mode (Supplement, p. 3, Fig. S1). The two OH measurement modes differ by the time used for the chemical conversion, 4 ms and 20 ms. Ratio of the signals with the short and the long conversion times may be used as an indicator of an artificial OH formation in the reactor (Kukui et al., 2008).

Measurements were performed by monitoring the peak intensities at m/z=62 (NO_3^-), m/z=97 ($H^{32}SO_4^-$), and m/z=99 ($H^{34}SO_4^-$) with the CIMS, respectively noted I_{62}, I_{97}, and I_{99} hereafter. Every measurement of OH was derived from 1 min of OH ion signal count and two 30 s background ion signal counts before and after the OH signal measurement. Peroxy radicals were measured at the end of the OH detection sequence by switching on the NO flow to the corresponding injector for a duration of 2 min. To avoid any possible influence of traces of NO on the OH measurements a time delay of 6 min was imposed after switching off the NO flow and before starting the next OH measurement sequence in order to ensure flushing of the CCR. The OH and the H_2SO_4 data were averaged resulting either in a sequence of 3 points with a step of 7 min separated by a time gap of 15 min or yielding a sequence with a time step of about 90 min. The latter was used to match the time resolution of the VOCs measurements (Supplement, p. 13, Table S4).

The concentration of OH and H_2SO_4 were derived from the measured ratios of the $H^{32}SO_4^-$, $H^{34}SO_4^-$ and NO_3^- ion peak intensities, I_{97}/I_{62} and I_{99}/I_{62}: [R] = $C_R \times I^R$, where R corresponds to OH or H_2SO_4, I^R is a combination of I_{97}/I_{62} and I_{99}/I_{62} ratios corresponding to OH or H_2SO_4 accounting for isotopic composition of SO_2 used for the chemical conversion (99% isotopic enrichment of ^{34}S, Eurisotop, Cambridge Isotope Laboratories, Inc.) and sulphur isotope natural abundance (^{32}S (95.02%) and ^{34}S (4.21%) (Hoefs, 2018)), C_R is a calibration coefficient determined in calibration measurements by production of OH or H_2SO_4 in a turbulent flow reactor using photolysis of water vapour at 184.9 nm and quantified by chemical actinometry using

photolysis of N_2O (Faloona et al., 2004). A detailed description of the calibration system with definitions of C_R and I^R are given in Supplement, pp. 4-12, Sect. S3.

The overall accuracy of the calibration coefficients was estimated taking into account uncertainties of all parameters used for calculation of the radical concentrations in the photolysis reactor and the precision of the measurements of the ratios I_{97}/I_{62} and I_{99}/I_{62}. The overall estimated calibration uncertainty (1σ) was of 30% for OH, 32% for H_2SO_4 and 8% for a ratio of $[H_2SO_4]$ to [OH], (Supplement, p. 12, Table S3). Accounting for the calibration uncertainties and the measurements precision, the overall 1σ uncertainty of the 14 min averaged measurements of OH, H_2SO_4 and the ratio of $[H_2SO_4]/[OH]$ was estimated to be around 32%, 34% and 16% during the daytime and 42%, 44% and 40% during the night time, respectively. During the ChArMEx/SAFMED campaign the observed level of OH background signal was significantly higher than typical OH background found during calibration or field measurements in air with low VOCs concentrations (see Fig. 7 and discussion in Sect. 4.4). Accordingly, the lower limits of detection at signal-to-noise ratio of 2 and a 15 min integration time were 2×10^5 molecule cm^{-3} for H_2SO_4 and 5×10^5 molecule cm^{-3} and 2×10^5 molecule cm^{-3} for OH daytime and nighttime measurements, respectively.

During the ChArMEx/SAFMED campaign the instrument was installed in a dedicated container with the CCR fixed to the roof of the container via an interface cap covered with a PTFE sheet. The sampling aperture of the reactor (3 mm diameter) was positioned 50 cm above the roof and about 3 m above the ground.

To avoid possible contamination of ambient air by the SO_2, NO and NO_2 reactants added to the CCR, a trap was set up at the pumps exhaust by using two 100 L cylinders containing zeolites. The cylinders were refilled several times during measurements. A flexible exhaust tube of 30 m length was always placed downwind from the container.

2.2.2 Complementary measurements

The aerosol particle size distribution was measured using a scanning mobility particle sizer (SMPS TSI 3080, associated with a CPC TSI 3010) in the range from 10.9 nm to 495.8 nm and with an aerodynamic particle sizer (APS, TSI 3321) in the range from 542 nm to 19.48 μm. As the SMPS measurements were made with dehydrated particles the particle diameters were corrected to ambient humidity using particle growth-factor (GF) of 1.5 at 90% determined with Volatility Hygroscopic— Tandem Differential Mobility Analyzer (VH-TDMA) (Villani et al., 2008). The dependence of the GF on relative humidity (RH) was calculated using the one-parameter approximation from Rissler et al. (2006). An estimated uncertainty of measured particle number densities and GF corrected particle diameters were of 10% and 15%, respectively.

SO_2 concentration was measured by UV fluorescence (Thermo Environmental Instruments (TEI), Model 43C-TLE) with an estimated accuracy of 20%, a lower detection limit of 0.05 ppb and a time resolution of 5 min.

Ozone concentration was measured by means of a CraNOx II (Eco Physics) NOx and O_3 monitor with an estimated accuracy of 10%.

A detailed description of VOCs measurements during ChArMEx/SAFMED campaign is given in Michoud et al. (2017). The measurements of 23 unsaturated VOCs including alkenes, aldehydes, ketones, isoprene and monoterpenes were used in

this work for estimation of SCIs concentrations. Employed measurement techniques and concentration ranges for measured unsaturated VOCs are given in Supplement, p. 13, Table S4 together with associated time resolution, limit of detection and uncertainties. The data were averaged or interpolated with a time step of 90 min.

Wind speed and direction, relative humidity, temperature and photolysis rates were also measured throughout the campaign.

2.3 Estimation of H2SO4 steady state concentrations

Concentrations of H_2SO_4 produced via SO_2 oxidation by OH and sum of SCIs, $H_2SO_4^{OH}$ and $H_2SO_4^{SCI}$, respectively, were calculated assuming validity of a steady state between the H_2SO_4 production and its loss (see discussion in Sect. 4.1),

$$[H_2SO_4]^{OH} = \frac{k_1 \cdot [OH] \cdot [SO_2]}{CS} \tag{1}$$

$$[H_2SO_4]^{SCI} = \frac{\left\{ \sum_i k_{SO2}^i \cdot [SCI^i] \right\} \times [SO_2]}{CS} \tag{2}$$

Here [OH] and [SO_2] are measured concentrations, [SCI^i] are estimated concentrations of speciated SCIs and CS, a condensation sink, is a rate of H_2SO_4 loss by its condensation on aerosol particles which is assumed to be the predominant H_2SO_4 loss process, while the dry deposition on macroscopic surfaces is neglected considering a long associated life time estimated of about 1 day using a typical deposition velocity of 1 cm s^{-1} (Seinfeld and Pandis, 2016) and boundary layer depth of 1 km. Considering the CS as a major sulfuric acid loss process the median value of H_2SO_4 lifetime was 2.7 min (2.2 min – 3.7 min interquartile range, Fig. 1, 2). The rate coefficient for the reaction of OH with SO_2, k_1=8.06×10^{-13} cm^3 molecule^{-1} s^{-1} (at 760 torr and 298 K), was taken from IUPAC 2004 recommendation (Atkinson et al., 2004) (see Discussion Sect.).

Production of $H_2SO_4^{SCI}$ is calculated as a sum of contributions from different speciated SCI^i reacting with SO_2 with rate coefficients k_{SO2}^i (Supplement, p. 15, Table S5). It is assumed here that the H_2SO_4 yield in reaction of SCIs with SO_2 is a unity for all SCIs, giving an upper limit for the contribution to H_2SO_4 formation of accounted SCIs.

The CS was calculated using measured particle size distributions and number concentrations by calculating diffusional flux to the aerosol particles assuming an accommodation coefficient of a unity (Hanson, 2005) and using Fuchs-Sutugin transition correction (Jefferson et al., 1998; Seinfeld and Pandis, 2016). Diffusion coefficient of H_2SO_4 was estimated using its dependence on relative humidity from Hanson and Eisele (2000) giving 0.077 cm^2 s^{-1} at RH of 60.6% (median value). Without considering an uncertainty on the accommodation coefficient, the accuracy of the calculated CS of 20% was assessed accounting for the uncertainties of particle measurements given in Sect. 2.2.2 and an uncertainty of H_2SO_4 diffusion coefficient of 5%.

Concentrations of speciated SCIs, [SCI^i], were calculated assuming steady state conditions considering their production by ozonolysis of the measured unsaturated VOCs and their loss by thermal decomposition and in reactions with water vapour (with H_2O and $(H_2O)_2$):

$$\left[\text{SCI}^i \right] = \frac{\left\{ \sum_X k_{X+O_3} \cdot \alpha_X^i \cdot Y_X^i \cdot [X] \right\} \times [O_3]}{K^i + k_{H_2O}^i \cdot [H_2O] + k_{(H_2O)_2}^i \cdot [(H_2O)_2]} \tag{3}$$

where X denotes a specific VOC, k_{X+O_3} is a rate coefficient for the reaction of X with O_3, α_X^i is a yield of stabilized SCI^i from CI^i, Y_X^i is a specific yield of CI^i in the reaction X+O$_3$, and K^i, $k_{H_2O}^i$, $k_{(H_2O)_2}^i$ are rate coefficients for the thermal decomposition, the reaction with H_2O and the reaction with water dimer for the specific SCI^i, respectively. Concentration of $(H_2O)_2$ was calculated using an equilibrium constant for water dimer formation and its temperature dependence from Ruscic (2013).

The rate coefficients and the yields α_X^i and Y_X^i for 36 SCIs derived from the ozonolysis of 23 measured VOCs are presented in Supplement Tables S4 (p. 13) and S5 (p. 15). Apart from a few rate coefficients and yields available from more recent experimental and theoretical studies, most of the parameters in Eq. (2) and Eq. (3) are taken from recommendations of Vereecken et al. (2017), which are grounded either on an analysis of available experimental data or derived from a theory based structure–activity relationships (SARs). For the 36 SCIs listed in Supplement Tables S4 (p. 13) and S5 (p. 15), we have adopted the SCIs naming convention from Vereecken et al. (2017). Uncertainty on the estimated in this way SCI concentrations is estimated in Vereecken et al. (2017) to be of an order of magnitude, mainly due to the uncertainties in CI speciation and the SCI decay rates.

3 Results

3.1 Observed data

Time series and median diel profiles of observed concentrations of OH, H_2SO_4, SO_2, O_3, selected VOCs and calculated condensation sink of H_2SO_4 are presented in Fig. 1 (time series) and Fig. 2 (median diel cycles, also including $J(O^1D)$, T, RH, and CS data). The night time OH and H_2SO_4 measurements on the 26 and 28-30 of July were influenced by strong fog event deteriorating the accuracy of the corresponding OH and H_2SO_4 data.

OH and H_2SO_4 concentrations reached around midday the maximum values of 4.3×10^6 molecule cm^{-3} and 8.5×10^6 molecule cm^{-3} (mean values for day time hours from 11:00 to 13:00 local time (= GMT + 2 h)), respectively, with night-time concentrations around 1×10^5 molecule cm^{-3} and 5×10^5 molecule cm^{-3} for OH and H_2SO_4, respectively, close to the detection limit.

Comparing the present observations (Fig. 2) with previous measurements in the Mediterranean region, the mean peak OH concentration during the noon hours was close to the peak OH levels observed during CYPHEX campaign in the summer of

2014 in Cyprus in the eastern Mediterranean, 5.8×10^6 molecule cm^{-3} (Mallik et al., 2018), where O_3 concentrations and $J(O^1D)$ peak levels were similar to those observed during ChArMEx ($J(O^1D)$ was measured during ChArMEx, but not yet published). The somewhat lower ChArMEx OH noon concentrations compared to CYPHEX are consistent with higher OH reactivity observed during ChArMEx (Zannoni et al., 2017), although the direct comparison of radical chemistry at these two sites is not straightforward considering that, among other differences between these sites, biogenic VOCs at Cyprus site, e.g. isoprene and monoterpenes, were 3-5 times lower compared to ChArMEx. About four times higher OH peak concentrations, 2.1×10^7 molecule cm^{-3}, were observed during the MINOS campaign in the summer of 2001 in Crete (central Mediterranean) with similar O_3 and $J(O^1D)$ observed levels (Berresheim et al., 2003). This difference is difficult to explain based on the available data (Mallik et al., 2018).
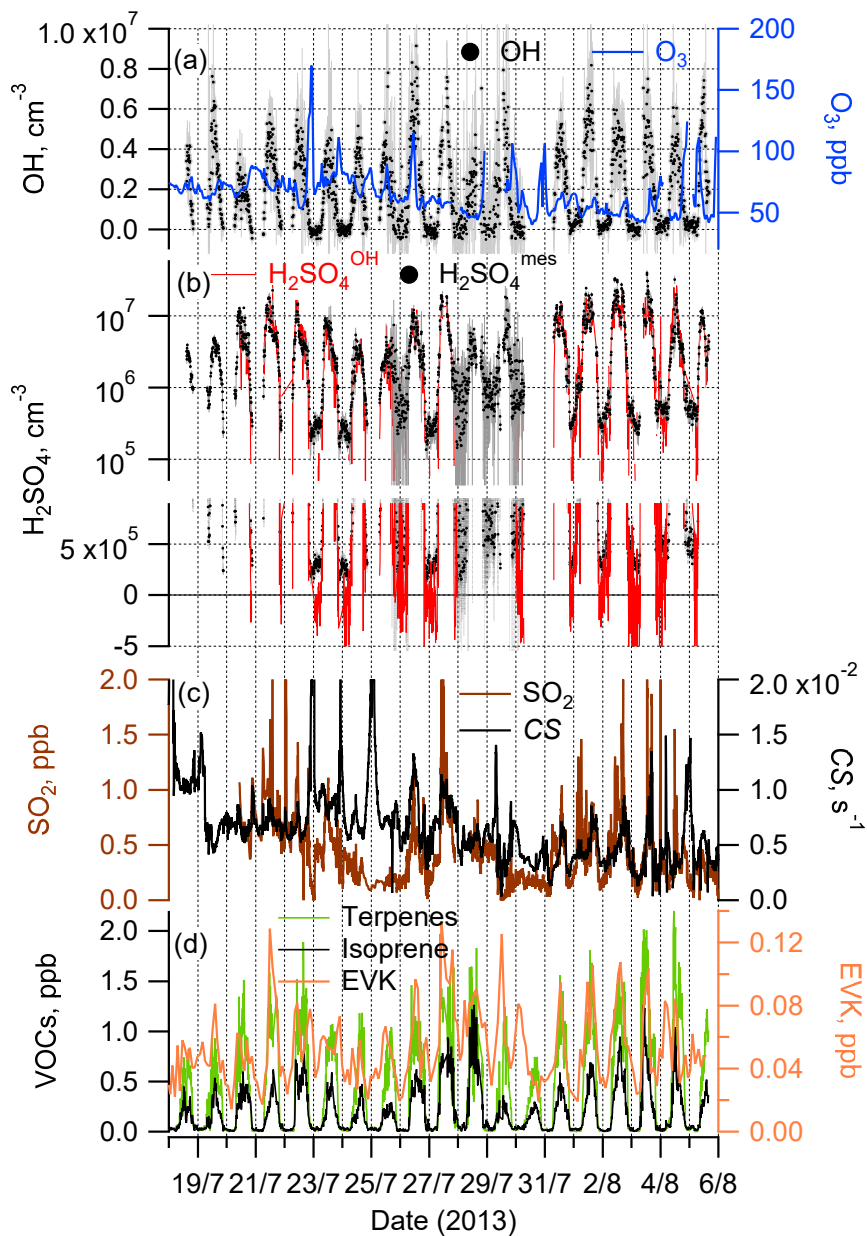
Figure 1. Time series of the observations during the ChArMEx summer 2013 campaign: OH radicals and O_3 (a); sulfuric acid observed, $H_2SO_4^{mes}$, and calculated assuming only SO_2+OH source, $H_2SO_4^{OH}$ (see Sect. 2.3) (b); SO_2 and condensation sink *CS* (c); total monoterpenes and isoprene (left axis), EVK (right axis) (d). For clarity, comparison of the measured $H_2SO_4^{mes}$ and calculated $H_2SO_4^{OH}$ concentrations is presented in (b) using two plots, with logarithmic and linear scales on the y-axis.

300

The observed ChArMEx H_2SO_4 concentrations were about two times higher than the observed OH concentrations. For other sites the observed ratios $[H_2SO_4]/[OH]$ were in the range from 1 to 9 with only one example when this ratio was less than unity (Supplement, p. 2, Table S1). The ratio $[H_2SO_4]/[OH]$ depends on the SO_2 concentration and condensation sink correlating with the aerosol particle surface area concentration. The condensation sink and $[SO_2]$ values during ChArMEx, with median values of 6.1×10^{-3} s^{-1} and 0.44 ppb, respectively, were typical for clean remote continental or coastal environments (Supplement, p. 2, Table S1).
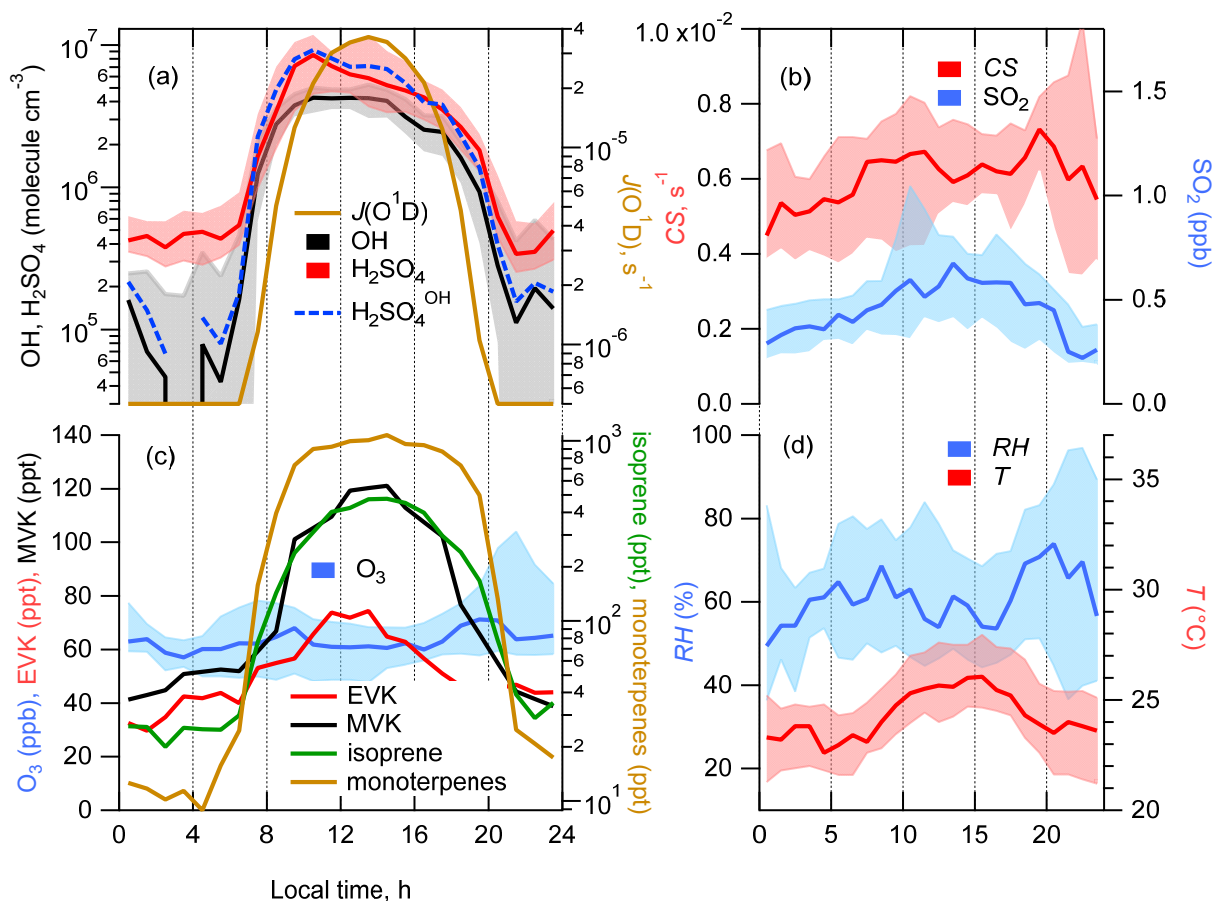
Figure 2. Median diel profiles of calculated $[H_2SO_4]$ produced in OH+SO_2 ($H_2SO_4^{OH}$), observed $[H_2SO_4]$, $[OH]$ and photolysis rate $J(O^1D)$ **(a)**, condensation sink (CS) and $[SO_2]$ **(b)**, $[O_3]$ and concentrations of selected VOCs **(c)**, relative humidity (RH) and temperature (T) **(d)**. Shaded areas represent the 25/75 percentiles.

The unsaturated VOCs observed during ChArMEx showed strong diel variation from about 0.4 ppb during the night to about 2 ppb at noon for the concentration of the sum of the VOCs (Fig. 1, 2, Supplement, p. 13, Fig. S9, Table S4). The major contribution during the day (from 7:00 to 20:00) was from biogenic VOCs (isoprene (22% on average), β-pinene (14%), α-

pinene (9%), α-terpinene (7%), methyl vinyl ketone (MVK) (5%) and methacrolein (MACR) (5%)) with emission rates correlating with temperature and solar radiation (Kesselmeier and Staudt, 1999). At night-time, the unsaturated VOCs were represented mostly by compounds of mixed biogenic and anthropogenic origin: ethene (31% on average), acrolein (14%) and ethyl vinyl ketone (9%). A significant night time contribution was also found from isoprene (9%) and its first-generation oxidation products MVK (6%) and MACR (6%).

3.2 Comparison of observed H_2SO_4 with sulfuric acid produced from $OH+SO_2$ ($H_2SO_4^{OH}$)

Time series of the H_2SO_4 produced in the reaction of OH with SO_2, $H_2SO_4^{OH}$, calculated according to Eq. (1) and of the observed H_2SO_4 are presented in Fig. 1b and 2b showing apparently good agreement between them during the day and an underestimation of the sulfuric acid concentration by $H_2SO_4^{OH}$ during the night. The inverse variance weighted mean value of the ratio of $[H_2SO_4]^{OH}/ [H_2SO_4]$ for the data presented in Fig. 1b is 0.86 ± 0.04 during the day (7:00 – 20:00) and 0.09 ± 0.02 during the night (20:00 – 7:00), respectively (Table 1). Uncertainties on the ratios $[H_2SO_4]^{OH}/[H_2SO_4]$ were estimated by accounting for the uncertainty on the measured ratio of $[OH]/[H_2SO_4]$ (see Sect. 2.2.1), on the SO_2 measurements (20%) and on the CS calculations (20%), without considering uncertainties on the reaction rate coefficient k_1 and the H_2SO_4 uptake coefficient (see Sect. 4.2 and Sect. 4.3).

Table 1. Comparison of observed $[H_2SO_4]$ with calculations assuming H_2SO_4 formation via oxidation of SO_2 by OH and SCIs. [OH] and $[H_2SO_4]$ are observed concentrations, $[H_2SO_4]^{OH}$ and $[H_2SO_4]^{SCI}$ are calculated H_2SO_4 produced by oxidation of SO_2 by OH and SCI, respectively. Values in square brackets correspond to $[H_2SO_4]^{OH}$ concentrations calculated with a rate coefficient for the reaction of OH with SO_2 from Medeiros et al. (2018) (see discussion in Sect. 4.2).

	Daytime: 7:00 – 20:00		Night-time: 20:00 – 7:00	
	Median (inter-quartile range)	Mean ± 1σ	Median (inter-quartile range)	Mean ± 1σ
[OH], 10^5 cm^{-3}	31 (18; 42)	31 ± 17	1.1 (-0.7; 3.0)	1.7 ± 4.0
$[H_2SO_4]$, 10^5 cm^{-3}	47 (28; 86)	63 ± 49	4.2 (3.1; 6.4)	5.8 ± 4.8
$[H_2SO_4]^{OH} = a + b \times [H_2SO_4]$	a=(-2.0±0.5)×10^5 ; b=0.85±0.02 [a=(-1.1±0.3)×10^5 ; b=0.52±0.01]		a=(-3.1±0.3)×10^5 ; b=0.97±0.1 [a=(-1.7±0.2)×10^5 ; b=0.60±0.05]	
$[H_2SO_4]^{OH}/ [H_2SO_4]$, %	95 (79; 129) [58 (48; 78)]	86 ± 4 [52 ± 2]	39 (-8; 84) [23 (-4; 52)]	9 ± 15~~2~~ [5 ± 9]
$1-[H_2SO_4]^{OH}/ [H_2SO_4]$, %	5 (-29; 21) [42 (22; 52)]	14 ± 4 [48 ± 2]	61 (16; 108) [77 (48; 104)]	91 ± 15~~2~~ [95 ± 9]
$[H_2SO_4]^{SCI}/ [H_2SO_4]$, %	10 (7; 16)	12 ± 6	30 (22; 48)	38 ± 24
$[H_2SO_4]-[H_2SO_4]^{OH}$, 10^5 cm^{-3}	1.2 (-12.5; 8.1) [15.2 (8.3; 36.5)]	4.6 ± 3.2 [11.2 ± 3.4]	3.0 (0.8; 5.2) [3.2 (1.8; 5.2)]	3.1± 0.4 [3.3 ± 0.3]
$[H_2SO_4]^{SCI}$, 10^5 cm^{-3}	6.0 (3.7; 8.6)	6.4 ± 3.7	1.4 (1.1; 2.4)	1.8 ± 1.2

Considering the correlation of the calculated sulfuric acid concentration $[H_2SO_4]^{OH}$ with the measured $[H_2SO_4]$ shown in Fig. 3, we find that the linear regression using a bivariate fit procedure accounting for the measurement errors of both H_2SO_4 and $H_2SO_4^{OH}$ (York et al., 2004) results in slopes of 0.85±0.02 and 0.97±0.1 for the daytime and the night-time, respectively. The linear regression yields significant intercepts of (-2.0±0.5) ×10^5 molecule cm^{-3} during the day and of (-3.1±0.3) ×10^5 molecule cm^{-3} at night. The close to unity slopes and the negative intercepts may be interpreted as a presence of an additional source contributing to H_2SO_4 on an average level of several of 10^5 molecule cm^{-3}. During the night this source is important comparing with the observed night-time average $[H_2SO_4]$ of (5.8 ± 4.8) ×10^5 molecule cm^{-3}. During the night the estimation of the contribution from missing sources derived from the linear fit is in qualitative agreements with the mean ratio of $[H_2SO_4]^{OH}$/$[H_2SO_4]$ of 0.09 indicating that the SO_2+OH source explains only about 10% of the H_2SO_4 formation. During day time, the reaction of SO_2 with OH source explains around 90% of the H_2SO_4 formation (Table 1).
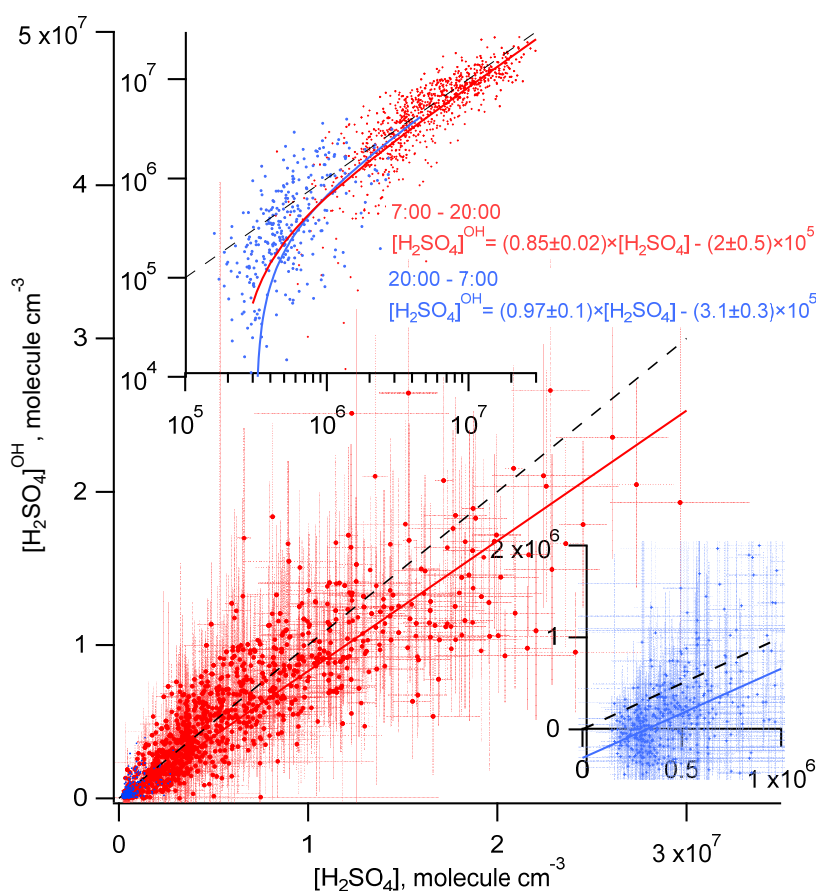
Figure 3. Comparison of the measured H_2SO_4 and the $H_2SO_4^{OH}$ calculated accounting only for the OH+SO_2 source during the day (red) and during the night (blue). Solid lines correspond to linear regression fitting accounting for both X and Y

measurement uncertainties. Dashed lines represent 1:1 ratios. Inserts, log-plot (upper) and linear plot (lower right), are added for clearer presentation of the night-time data.

3.3 Comparison of observed H_2SO_4 with sulfuric acid produced from SCIs+SO$_2$ ($H_2SO_4^{SCI}$)

355   Estimated according to Eq. (2) and (3), mean diel profiles of the sulphuric acid $H_2SO_4^{SCI}$ produced in the reactions of SO_2 with SCIs generated by the ozonolysis of the measured unsaturated VOCs, excluding α-terpinene, are presented in Fig. 4a. The calculated contribution from α-terpinene alone is up to six times larger than observed [H_2SO_4] (Fig. 4b). It is not clear if the reason for this large overestimation can be related to an erroneous α-terpinene measurements and/or to incorrect kinetic parameters used for the calculation of H_2SO_4 production from α-terpinene. The observed α-terpinene daytime concentrations

360   were similar to the concentrations of α-pinene and β-pinene. Accounting for about 100 times faster α-terpinene consumption in reactions with OH and O_3 compared to other terpenes (Atkinson et al., 2006; IUPAC, 2020) that would imply about 100 times larger α-terpinene emission rate at the measurement site, which is unlikely considering observed compositions of monoterpene emissions of biogenic origin (Geron et al., 2000). Being well outside of the uncertainty of the H_2SO_4 measurements the contribution from α-terpinene was therefore excluded from consideration in this work.

365
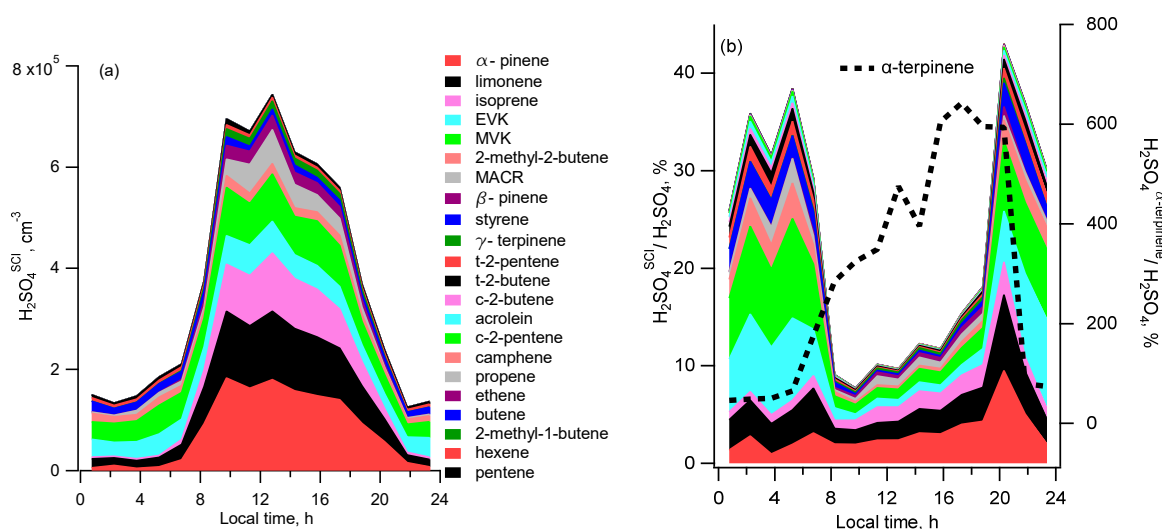
Figure 4. Diel profiles of the mean calculated H_2SO_4 concentrations produced from ozonolysis of different VOCs: (a) - filled regions correspond to [H_2SO_4]^{SCI} produced by ozonolysis of different VOCs; (b) - profiles of ratios of [H_2SO_4]^{SCI} from different VOCs to the measured [H_2SO_4]. Black dotted line in (b) corresponds to [H_2SO_4]^{SCI} produced by the ozonolysis of α-terpinene

370   (right axis).

The calculated concentration of the sum of $H_2SO_4^{SCI}$ reaches a maximum of about 7×10^5 molecules cm^{-3} around midday and goes down to about 1.5×10^5 molecules cm^{-3} during the night. The largest estimated contribution to the $H_2SO_4^{SCI}$ is from α-pinene, limonene and isoprene during the day and from MVK and EVK at the night-time (Fig. 4).

375   The largest contribution to the calculated sum of SCIs was from the *syn* form of acetaldehyde oxide, Z-CH_3CHOO (2), E-MVK-oxide (10) from isoprene, oxo-substituted E-(C(O)R)CHOO (31) (with R=H, CH_3, and C_2H_5 for the SCI from acrolein, MVK and EVK, respectively), phenyl-substituted carbonyl oxide PhCHOO (35) from styrene and Z-pinonaldehyde-K-oxide (13) from α-pinene (the SCIs numbering given in parenthesis corresponds to the SCIs numbering in Supplement Tables S4 (p. 13) and S5 (p. 15).

380   15)). The night-time and the daytime mean concentrations of the sum of all SCIs were about 10^3 molecule cm^{-3} and 3×10^3 molecule cm^{-3}, respectively. *Z*-pinonaldehyde-K-oxide (13) (from α-pinene) and E-(C(O)R)CHOO (31) (from MVK, EVK and acrolein) were also the major SCIs producing H_2SO_4. In addition, comparable contribution to H_2SO_4 formation was from *Z*-(CHR_aR_b)(CH_3)COO (21) (from limonene ozonolysis) and *E*-MVK-oxide (10) (from isoprene ozonolysis). Detailed information is given in Supplement, p. 16, Fig. S10.

385
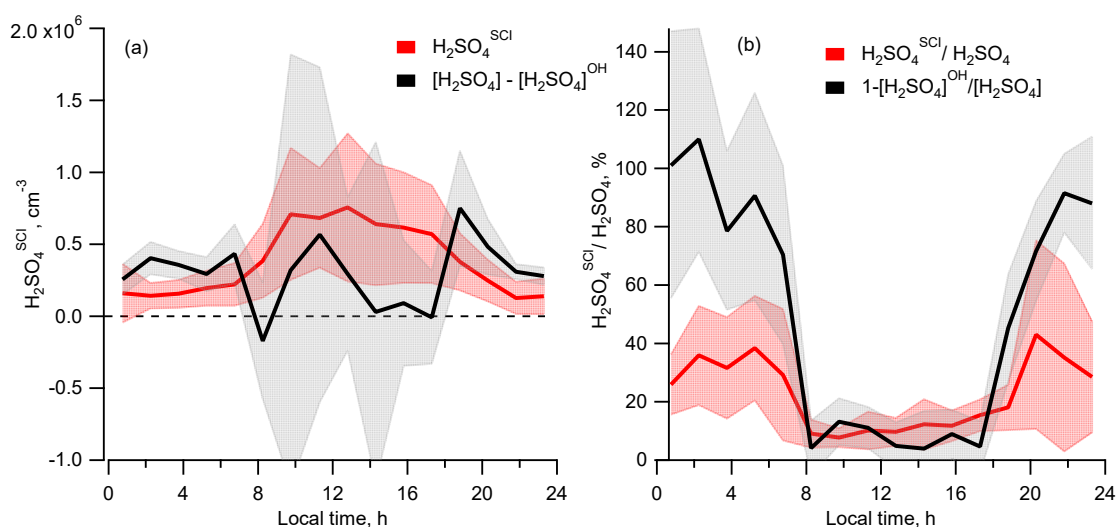
Figure 5. Comparison of the sulfuric acid produced by oxidation of SO_2 by SCIs, $H_2SO_4^{SCI}$, and missing source of H_2SO_4 derived from the difference of the measured $[H_2SO_4]$ and $[H_2SO_4]^{OH}$. (a) Diel profiles of the mean $[H_2SO_4]^{SCI}$ (red) and $[H_2SO_4]-[H_2SO_4]^{OH}$ (black). (b) Diel profiles of the mean of the relative contributions $[H_2SO_4]^{SCI}/[H_2SO_4]$ (red) and $1-[H_2SO_4]^{OH}/[H_2SO_4]$ (black). Shaded areas correspond to $\pm 1\sigma$ standard deviation.

Comparing the calculated $[H_2SO_4]^{SCI}$ with the missing H_2SO_4 source derived from the difference of the measured $[H_2SO_4]$ and calculated $[H_2SO_4]^{OH}$, Fig. 5a shows that compared to the difference of $[H_2SO_4] - [H_2SO_4]^{OH}$ representing the missing H_2SO_4 source, the $[H_2SO_4]^{SCI}$ is lower during the night and higher during the day with a difference of several 10^5 molecule

cm^{-3} (Table 1). The large variance of the average [H$_2$SO$_4$] - [H$_2$SO$_4$]^{OH} difference presented in Table 1 is due to the large scattering of these values derived either from a small difference of large OH and H$_2$SO$_4$ signals or from the measurements of OH and H$_2$SO$_4$ concentrations close to their lower detection limits, as well as due to a stochastic day to day natural variation.

Shown in Fig. 4b, the calculated dial profile of the relative H$_2$SO$_4^{SCI}$ to H$_2$SO$_4$ contribution resembles the dial profile of a missing H$_2$SO$_4$ source derived from the relative concentration difference of H$_2$SO$_4$ and H$_2$SO$_4^{OH}$, i.e. 1-[H$_2$SO$_4$]^{OH}/[H$_2$SO$_4$]. Both profiles exhibit a shallow well from about 8:00h to 18:00h during the day with higher relative contribution during the night. According to the [H$_2$SO$_4$]^{SCI} calculations, the SCIs contribution is about three times higher during the night constituting (38±24)% compared to (12±6)% during daytime. The calculated [H$_2$SO$_4$]^{SCI} contribution is significantly lower than the night-time missing source of (91±2)% and is in good agreement with the missing (14±4)% during the day (Table 1). The large unexplained formation of H$_2$SO$_4$ during the night can be related to the large uncertainty on the calculated SCI concentrations and the rates of H$_2$SO$_4$ production from their reactions with SO$_2$ (Vereecken et al., 2017), as well as to an unaccounted contribution from the ozonolysis of some unsaturated compounds not measured during the campaign. The latter explanation is supported by a significant daytime and night-time missing OH reactivity of about 50%, observed by Zannoni et al. (2017) during ChArMEx using the same VOCs data as in the present work. The main unaccounted species were suggested to be reactive biogenic VOCs including sesquiterpenes, oxygenated terpenes and their oxidation products. Ozonolysis of these compounds could be an additional unaccounted source of SCI in the present work.

4 Discussion

4.1 Validity of H$_2$SO$_4$ steady state conditions

Estimated concentrations of H$_2$SO$_4$ produced in reactions of SO$_2$ with OH and with SCIs are based on the assumption of a steady state between production and loss pathways of H$_2$SO$_4$. All variations of the parameters influencing the H$_2$SO$_4$ concentration in the air masses incoming to the measurements site are assumed to occur on a time scale that is longer than the lifetime of H$_2$SO$_4$ estimated on the basis of the local aerosol measurements. These conditions are not obviously fulfilled at the Ersa site because the air masses arriving at the island may become influenced by local biogenic emissions, possibly leading to varying concentrations of these compounds along the trajectory from the coast to the measurement location (due to non-uniformly distributed emissions, development of vertical profile of VOCs and other reasons). As the production rate of the SCIs is proportional to the corresponding concentrations of the unsaturated compounds the variation of VOCs may induce variations in the SCIs concentrations. The concentration of OH could also be affected by varying VOCs concentrations considering that the lifetime of OH at the measurements site was about 0.2 s with half of the OH reactivity explained by the local biogenic emissions (Zannoni et al., 2017).

The steady state conditions were hardly disturbed by variations of the concentrations of SO$_2$ and O$_3$, species of non-local origin with the lifetime longer than the lifetime of H$_2$SO$_4$. Concerning the H$_2$SO$_4$ condensation sink, a variation in the aerosol particle number concentration and size distribution could be present. Recent studies evidenced that highly oxygenated

molecules (HOMs) from the ozonolysis of monoterpenes may initiate new particle formation and its fast initial growth with the growth rates of tens of nm per hour (Stolzenburg et al., 2018; Tröstl et al., 2016). However, these variation are still slow compared to the H_2SO_4 lifetime of several minutes.

430   The time scales for the variations of VOCs, SCI, OH and CS may depend on the distribution of the biogenic emissions, wind speed, conditions of turbulent mixing and others. Without information about all these details we can only estimate the maximum time for such variations corresponding to the time of air masses presence over the land. To fulfill the steady state conditions this presence time has to be at least longer than the lifetime of H_2SO_4. The prevailing wind directions were from the NE and, predominantly, from the SW. The SW direction corresponds to the shortest presence times because of the shortest

435 distance to the coastline and the highest wind speeds corresponding to this wind directions (Supplement, p. 17, Fig. S11, S12). On average, the presence time over the land, t_{pr}, significantly exceeded the H_2SO_4 lifetime, t_{H2SO4}, with the median value of the ratio of t_{pr} / t_{H2SO4} being of 7.7 (4.3 – 17.9 interquartile range). To test an influence of the presence time on the calculated H_2SO_4 budget, the dependencies between the relative difference $1-[H_2SO_4]^{OH}/[H_2SO_4]$ and the relative contribution $[H_2SO_4]^{SCI}/[H_2SO_4]$ were analyzed with a filtered data using criteria $t_{pr} / t_{H2SO4} > 1$ and $t_{pr} / t_{H2SO4} > 10$. No significant

440 difference were found compared with the unfiltered data, as it is also illustrated in Fig. 6 showing no apparent correlation between the relative contribution of the $OH+SO_2$ source and the ratio of t_{pr} / t_{H2SO4}. Similarly, no apparent effect was found by filtering the data according to the wind speed and the wind direction (not presented). Finally, although relatively short time scale spatial variability of OH or SCIs concentrations around the measurement site cannot be excluded, an apparent independence on the presence time or the wind speed support the validity of the assumption used here regarding H_2SO_4 steady

445 state conditions.
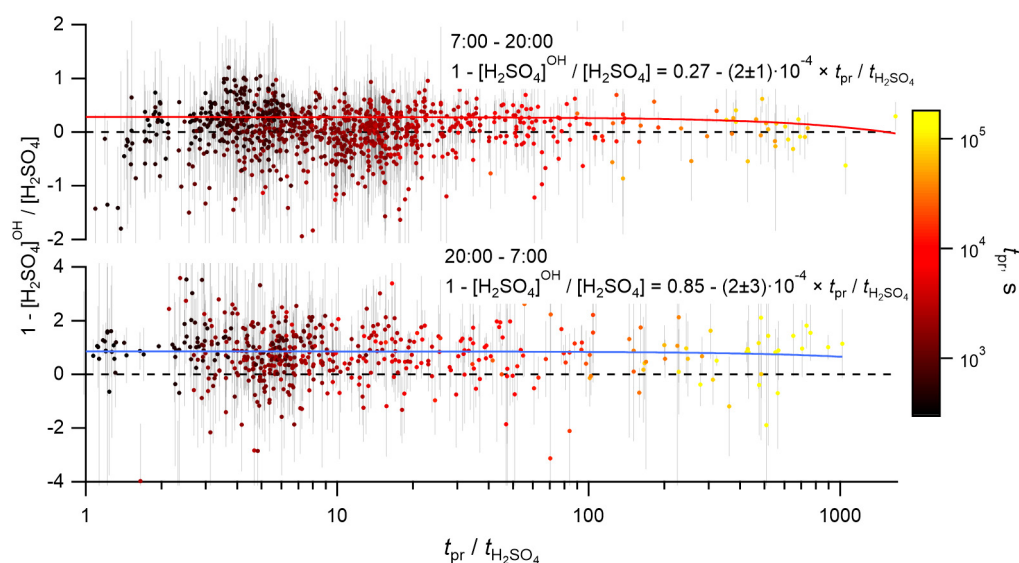
Figure 6. Dependence of the normalized difference of the H_2SO_4 concentrations observed and produced from SO_2+OH, $1-[H_2SO_4]^{OH}/[H_2SO_4]$, on the ratio of presence time over the land to the lifetime of H_2SO_4, t_{pr} / t_{H2SO4}, colored by the presence

time over the land, t_{pr}. Upper and lower figures correspond to the daytime and the night-time data, respectively. Solid lines correspond to linear regression fits.

4.2 OH+SO$_2$ reaction rate constant

In this work the rate coefficient for the reaction of OH with SO$_2$, k_1=8.06×10^{-13} cm^3 molecule^{-1} s^{-1} (at 760 torr and 298 K), was taken from the last published IUPAC recommendation (Atkinson et al., 2004). The two latest JPL evaluations recommend an about 20% larger rate constant of 9.6×10^{-13} cm^3 molecule^{-1} s^{-1} (Burkholder et al., 2015, 2019). Using the rate constant from the JPL evaluations in this work would result in about 20% larger H$_2$SO$_4$ production rate via OH+SO$_2$. This would yield a closed H$_2$SO$_4$ budget with only OH+SO$_2$ source during the day and about two times lower contribution from a missing source during the night.

In a recent study of Blitz et al. (2017a, 2017b) a significantly lower rate constant of 5.8×10^{-13} cm^3 molecule^{-1} s^{-1} was derived from experiments with vibrationally excited OH (v=1,2,3)+SO$_2$ and using the master equation analysis of the pressure and temperature dependence of their own and some others experimental OH+SO$_2$ reaction rate constants. An even lower rate constant of 4.8×10^{-13} cm^3 molecule^{-1} s^{-1} has been derived by Medeiros et al. (2018) applying more detailed master equation analysis of experimental data from Blitz et al. (2017a, 2017b) and some other data. These recent results have not been confirmed by other studies. Also, they have been discussed but not ~~included~~ recommended ~~in~~ by the latest JPL evaluation (Burkholder et al., 2019).

Using the lower rate constant from Medeiros et al. (2018) in our study would result in about 2 times reduced H$_2$SO$_4$ production by oxidation of SO$_2$ by OH and would invoke either significantly larger contribution from an additional H$_2$SO$_4$ source or a lower H$_2$SO$_4$ uptake coefficient, of about 0.5 instead of unity. As shown in Table 1, the reaction of OH with SO$_2$ would explain only about 50% and 5% of the observed H$_2$SO$_4$ production during the day and during the night, respectively.

In previous field studies of the H$_2$SO$_4$ budget listed in Supplement, p. 2, Table S1, the OH+SO$_2$ production rate of H$_2$SO$_4$ was calculated using k_1 rate coefficient in the range of (8.5 – 12) × 10^{-13} cm^3 molecule^{-1} s^{-1}. Reanalysis of these data using the lower k_1 would lead to a conclusion that the H$_2$SO$_4$ budget was never observed to be closed with the uptake coefficient close to unity. On the other hand, the employing the lower k$_1$ from Blitz et al. (2017a, 2017b) in model studies results in a significantly larger relative contribution of SCI to the H$_2$SO$_4$ formation. For example, the SCI contribution of 7% in a rural environment and of 70% in tropical regions, which were estimated assuming the lower k$_1$ by Vereecken et al. (2017), would be reduced respectively to negligible and to about 30%, if the larger k$_1$ from IUPAC or JPL was used.

4.3 H$_2$SO$_4$ loss

The mass accommodation coefficient of unity used in this work was measured by Hanson (2005) for the H$_2$SO$_4$ uptake on 5 - 20 nm diameter particles composed of water and sulfuric acid. The efficient uptake of H$_2$SO$_4$ is supported by other studies where the accommodation coefficients of about 0.7 were determined for the uptake on liquid sulfuric acid (Pöschl et al., 1998) and on ammonium sulfate and sodium chloride particles (Jefferson et al., 1997). Lower mass accommodation coefficients in

the range of 0.2-0.3 were determined for the uptake on hydrocarbon coated particles (Jefferson et al., 1997) suggesting that the uptake coefficient may depend on aerosol composition. Considering the measurements uncertainty, the results obtained in this work are consistent with the accommodation coefficient in the range from about 0.8 to 1. At lower uptake values the $OH+SO_2$ source would significantly override the calculated H_2SO_4 loss during the day. At the same time, the apparently missing H_2SO_4 source during the night can be explained by a lower uptake coefficient, down to about 0.5.

Another possible loss mechanism of H_2SO_4 can be via collisions of sulfuric acid molecules leading to new particles formation (NPF) in the atmosphere. For some atmospheric conditions like in the presence of high concentrations of base atmospheric components, e.g. ammonia and amines (Almeida et al., 2013), stabilizing the H_2SO_4 dimer and larger clusters, the nucleation may proceed at collisionaly limited rate corresponding to an effective bimolecular H_2SO_4 loss rate coefficient of about 4×10^{-10} cm^3 $molecule^{-1}$ s^{-1} (Kürten et al., 2014). Such conditions might have been encountered in highly polluted industrial and urban environments, regions influenced by strong agricultural emissions, and in chamber experiments (Kürten et al., 2016, 2018; Yao et al., 2018). Removal of H_2SO_4 with this rate constant would significantly contribute to its loss during ChArMEx, increasing it by about a factor of 2 for the largest observed H_2SO_4 concentrations. During the ChArMEx/SAFMED experiment, the H_2SO_4 loss rate assuming sulphuric acid initiated kinetic particle formation can be estimated from several episodes of the NPF observed during the campaign (on days from 29/07 to 2/09; (Berland et al., 2017)). Supplement, p. 18, Fig. S13 shows example of NPF observed around midday of the 31st of July. For this day the profiles of H_2SO_4 and N_{10-15} are similar with a time delay of about 2 hours for the maximum of the size distribution of 15 nm. This allows us to assume that the observed NPF on this day could be related to the evolution of the H_2SO_4 concentration. The growth rates (GR) and 12 nm particle apparent formation rates from the SMPS measurements are 3.1 nm h^{-1} and 8.2×10^{-3} cm^{-3} s^{-1}, respectively. GR was calculated using a maximum-concentration method (Kulmala et al., 2012). Using the approach of Kerminen and Kulmala (2002) and Sihto et al. (2006) to derive the rate of formation of critical cluster of size 1 nm, J_1, we obtain around 1 cm^{-3} s^{-1} at H_2SO_4 concentration of around 10^7 molecule cm^{-3}. Assuming kinetically limited nucleation mechanism in which the critical cluster contains two sulfuric acid molecules, this corresponds to the bimolecular rate constant of 5×10^{-13} for the removal of H_2SO_4, which would correspond to a negligible H_2SO_4 loss compared to the condensation on existing particles. Similar rates, several orders of magnitude below the collision limited rate, were found in other diverse continental and marine atmospheric environments (Kuang et al., 2008). Besides, the GR estimated from the time delay between H_2SO_4 profile and corresponding increase in N_{10-15} particles is about 2 times faster than derived from the particle size growth rate. Using this latter GR would result in an even slower particle formation. Finally, analysis of particles origin and their chemical composition at the measurement site made with ATOMF MS indicate that even if the traces of amines were present they were of remote origin and not present on the measurement site (Arndt et al., 2017).

4.4 SCIs interference with OH and H_2SO_4 measurements

High concentrations of SO_2 used in the chemical conversion reactor of CIMS instruments for the conversion of OH into H_2SO_4 may lead to an interference with OH and H_2SO_4 measurements due to an artificial generation of H_2SO_4 in reactions of

SCIs with SO_2 inside the reactor. When the reactant used as a scavenger of OH does not react fast with SCIs, e.g. using propane, the contribution of the artificially formed H_2SO_4 is the same for the OH measurements in the background (BG) and the OH signal + background modes (OH+BG), if the SO_2 injection position rests unchanged for the measurements in both modes. In this case the OH signal derived from the difference of the OH+BG and the BG signals is free from the artificial H_2SO_4 formation. However, the presence of an additional SO_2 oxidant not efficiently removed by OH scavenger may lead to a significant increase of the BG level as it was observed in previous field measurements (Berresheim et al., 2014; Mauldin III et al., 2012).

In the instrument used in this study the OH is scavenged with NO_2. The rate constant for the reaction of NO_2 with CH_2OO, CH_3CHOO and $(CH_3)_2COO$ stabilized CIs was found to be of about 2×10^{-12} cm^3 molecule^{-1} s^{-1} (Chhantyal-Pun et al., 2017; Stone et al., 2014; Taatjes et al., 2013), which is about $10 - 100$ times smaller than typical rate constants of the reactions of SCIs with SO_2 (Supplement, p. 15, Table S5). As the ratio of $[NO_2]/[^{34}SO_2]$ in the reactor was about 100, the SCIs in the reactor may react with similar rates with both SO_2 and NO_2 contributing to the BG signal. In addition, as the NO_2 and SO_2 injection positions are different for the BG and OH+BG modes (see Supplement, p. 3, Fig. S1 for details), the OH signal derived from the OH+BG and the BG difference may also be influenced by the artificial $H_2^{34}SO_4$ production in reactions of SCIs with SO_2.

As presented in Fig. 7, the BG signal observed during ChArMEx showed a diel profile similar to that of VOCs or OH (Fig. 1 and 2) with maximum at noon and minimum during the night. The peak noon and night-time BG signals reached levels corresponding to OH concentrations of about 5×10^6 molecule cm^{-3} and 1×10^6 molecule cm^{-3}, respectively. These BG levels are significantly higher than values of about $(1 - 5) \times10^5$ molecule cm^{-3} typically observed with the present instrument during calibration with Zero air or during measurements in clean air with low VOCs concentrations, e.g. in Antarctica (Kukui et al., 2014).
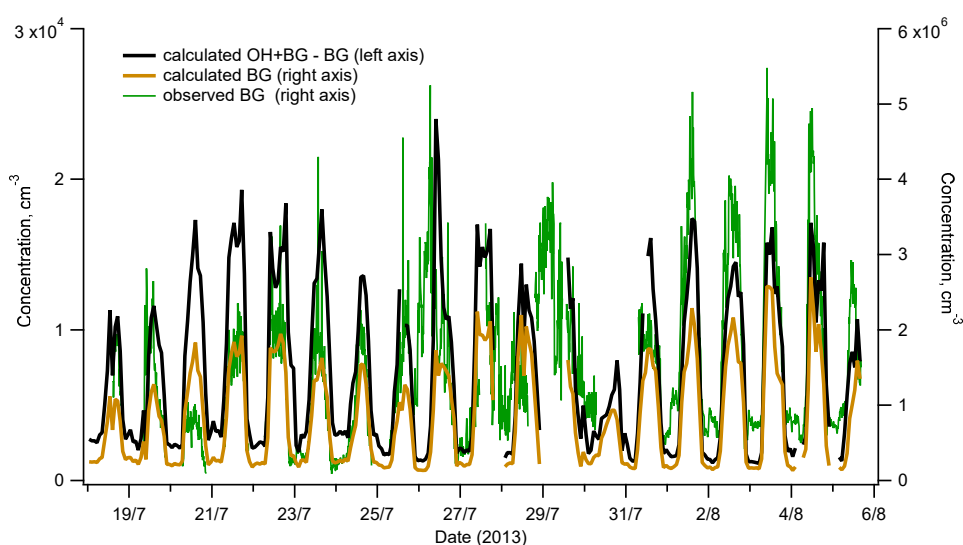
Figure 7. Interference with OH measurements from the H_2SO_4 produced in the reactor by reactions of SO_2 with SCIs: calculated contribution to measured OH (red line, left axis) and comparison of the observed background (BG) (blue line, right axis) and the BG calculated assuming its origin from the reactions of SCIs with SO_2 inside the reactor (black line, right axis).

To examine if the observed high BG levels can be explained by the SO_2 reaction with SCIs the H_2SO_4 concentration produced in the reactor in reactions of the sum of SCIs with SO_2, $[H_2{}^{34}SO_4]^{SCI/R}$, was calculated for BG and OH+BG modes using Eq. (4), which is similar to Eq. (2) but neglects the H_2SO_4 losses in the reactor:

$$\left[H_2{}^{34}SO_4\right]^{SCI/R} = \sum_{R_j}\left\{\sum_i k_2^i \cdot \left[SCI^i\right]^{R_j}\right\} \times \left[{}^{34}SO_2\right]^{R_j} \times t_{R_j}, \qquad (4)$$

where the index R_j corresponds to different parts of the reactor, $\left[SCI^i\right]^{R_j}$ and $\left[{}^{34}SO_2\right]^{R_j}$ are the concentrations and t_{R_j} is the bulk flow time in the corresponding parts of the reactor (see also Supplement, p. 3, Fig. S1). The concentrations of SCIs inside the reactor generated by ozonolysis of the measured unsaturated VOCs were calculated similarly to Eq. (3) but with accounting for the additional SCIs loss in reactions with SO_2 and NO_2 injected into the reactor. The concentrations of VOCs, O_3 and H_2O inside the reactor were calculated using the ambient measurements with accounting for a dilution inside the reactor.

The concentration of O_3 in the IMR was corrected by accounting for ozone generated in the corona discharge ion source and added to the IMR with the flow of primary ions. Amount of O_3 generated by the ion source depends on the ion source operating configuration, i.e., flow rates of injected mixtures, composition of the mixtures and potentials of the ion source electrodes. The concentration of O_3 in the IMR was not monitored during the campaign, but according to later checks this concentration was of 2 ± 1 ppm and this value was used for the estimation of $[H_2{}^{34}SO_4]^{SCI/R}$.

As shown in Fig. 7, the calculated and the observed BGs exhibit similar variability and correspond to comparable concentration levels allowing us to suggest that the observed elevated BG levels were related to the SO_2 oxidation by SCIs in the reactor. This hypothesis is supported by results of later experiments on the ozonolysis of terpenes conducted in an environmental chamber where a strong dependence of the observed BG level on the SCIs production rate was confirmed, as shown in Supplement, p. 19, Fig. S14 for the ozonolysis of α-pinene.

Concerning a possible interference of the SO_2+SCIs reaction with the OH measurements, Fig. 7 shows that during the campaign, this interference was negligible because the difference of $[H_2{}^{34}SO_4]^{SCI/R}$ produced in the OH+BG and the BG modes corresponded to OH concentration lower than 2×10^4 molecule cm^{-3}, about 10 times lower than the OH lower detection limit. Notably, this contribution is independent on the $[O_3]$ in the IMR influencing equally the OH+BG and BG measurements.

5 Conclusions

The formation of H_2SO_4 was observed at the Ersa station in northern Corsica, a site influenced by local emissions of biogenic VOCs. The H_2SO_4 concentration reached 10^7 molecule cm^{-3} at midday and was around 5×10^5 molecule cm^{-3} during

the night. Based on the OH, H_2SO_4, SO_2 and particle number density measurements and assuming validity of a steady state between H_2SO_4 production and its loss by condensation on existing aerosol particles with a unity accommodation coefficient, we have found that the contribution of the SO_2 + OH reaction accounts for (86 ± 4) % and only for (9 ± 2) % of the H_2SO_4 production during the day and night, respectively. The given accuracy of these values has been estimated without accounting for the large uncertainty in the OH + SO_2 reaction rate coefficient, which results in a larger uncertainty in the derived here contribution to H_2SO_4 formation from the OH+SO_2 source, from about a factor of 1.5 its overestimation to about 20% its underestimation.

Estimating the H_2SO_4 production from the SO_2 oxidation by SCIs, we conclude that despite the low calculated SCIs concentrations $((1-3) \times 10^3$ molecule cm^{-3} for the sum of SCIs), this source may explain about 10% of the H_2SO_4 formation during the day and represents a major source of H_2SO_4 accounting for about 40% of its formation during the night. The sum of the H_2SO_4 production rates via SO_2+OH and SO_2+SCIs correspond to a closure of the H_2SO_4 budget during the day, but seem to underestimate by 50% the H_2SO_4 production during the night, with the latter being possibly related to uncertainties in the used in this work kinetic parameters, an unaccounted contribution from the ozonolysis of some unsaturated compounds not measured during the campaign, as well as to some yet unidentified H_2SO_4 production mechanisms during night-time.

Both the daytime and night-time results of this study indicate that the oxidation of SO_2 by SCIs may be an important source of H_2SO_4 in VOCs-rich environments, especially during night-time.

Author's contributions

AK designed the CIMS instrument, performed the OH and H_2SO_4 measurements, analyzed the data and wrote the paper. MC participated in the design of the new calibration system. All other coauthors participated in data collection. All coauthors participated in paper discussion.

Competing interests

The authors declare that they have no conflict of interest

Data availability

Data is available upon request from the authors.

Acknowledgements

The authors would like to thank Thierry Vincent, Stephane Chevrier and Gilles Chalumeau from LPC2E for logistical help in preparation and during the campaign, Karine Sartelet from CEREA for managing the SAFMED project, Jean Sciare from

595   LSCE (now at CyI) for managing the campaign site and providing meteorology data, Eric Hamonou and François Dulac from LSCE for organizing the ChArMEx campaign and for managing and coordinating the ChArMEx project, François Dulac for editorial corrections and suggestions.

Financial support

This research has received funding from the French National Research Agency (ANR) projects SAFMED (grant ANR-12-BS06-0013). This work is part of the ChArMEx project supported by ADEME, CEA, CNRS-INSU and Météo-France through

600   the multidisciplinary program MISTRALS (Mediterranean Integrated Studies aT Regional And Local Scales). The station at Ersa was partly supported by the CORSiCA project funded by the Collectivité Territoriale de Corse (CTC) through the Fonds Européen de Développement Régional of the European Operational Program 2007–2013 and the Contrat de Plan Etat-Région. This project was also supported by the CaPPA project (Chemical and Physical Properties of the Atmosphere), funded by the French National Research Agency (ANR) through the PIA (Programme d'Investissement d'Avenir) under contract ANR-11-

605   LABX-0005-01 and by the Regional Council Nord-Pas de Calais and the European Funds for Regional Economic Development (FEDER). This work was also supported by the LABEX VOLTAIRE ANR-10-LABX-100-01 (2011–20) and the PIVOTS project provided by the Région Centre—Val de Loire (ARD 2020 program and CPER 2015–2020).

References

Ahrens, J., Carlsson, P. T. M., Hertl, N., Olzmann, M., Pfeifle, M., Wolf, J. L. and Zeuch, T.: Infrared detection of Criegee

610   intermediates formed during the ozonolysis of β-pinene and their reactivity towards sulfur dioxide, Angew. Chemie - Int. Ed., 53(3), 715–719, doi:10.1002/anie.201307327, 2014.

Almeida, J., Schobesberger, S., Kürten, A., Ortega, I. K., Kupiainen-Määttä, O., Praplan, A. P., Adamov, A., Amorim, A., Bianchi, F., Breitenlechner, M., David, A., Dommen, J., Donahue, N. M., Downard, A., Dunne, E., Duplissy, J., Ehrhart, S., Flagan, R. C., Franchin, A., Guida, R., Hakala, J., Hansel, A., Heinritzi, M., Henschel, H., Jokinen, T., Junninen, H.,

615   Kajos, M., Kangasluoma, J., Keskinen, H., Kupc, A., Kurtén, T., Kvashin, A. N., Laaksonen, A., Lehtipalo, K., Leiminger, M., Leppä, J., Loukonen, V., Makhmutov, V., Mathot, S., McGrath, M. J., Nieminen, T., Olenius, T., Onnela, A., Petäjä, T., Riccobono, F., Riipinen, I., Rissanen, M., Rondo, L., Ruuskanen, T., Santos, F. D., Sarnela, N., Schallhart, S., Schnitzhofer, R., Seinfeld, J. H., Simon, M., Sipilä, M., Stozhkov, Y., Stratmann, F., Tomé, A., Tröstl, J., Tsagkogeorgas, G., Vaattovaara, P., Viisanen, Y., Virtanen, A., Vrtala, A., Wagner, P. E., Weingartner, E., Wex, H.,

620   Williamson, C., Wimmer, D., Ye, P., Yli-Juuti, T., Carslaw, K. S., Kulmala, M., Curtius, J., Baltensperger, U., Worsnop, D. R., Vehkamäki, H. and Kirkby, J.: Molecular understanding of sulphuric acid–amine particle nucleation in the atmosphere, Nature, 502, 359–363, doi:10.1038/nature12663, 2013.

Arndt, J., Sciare, J., Mallet, M., Roberts, G. C., Marchand, N., Sartelet, K., Sellegri, K., Dulac, F., Healy, R. M. and Wenger,

J. C.: Sources and mixing state of summertime background aerosol in the north-western Mediterranean basin, Atmos.

625   Chem. Phys., 17, 6975–7001, doi:10.5194/acp-17-6975-2017, 2017.

Atkinson, R., Baulch, D. L., Cox, R. A., Crowley, J. N., Hampson, R. F., Hynes, R. G., Jenkin, M. E., Rossi, M. J. and Troe, J.: Evaluated kinetic and photochemical data for atmospheric chemistry: Volume I - gas phase reactions of O_x, HO_x, NO_x and SO_x species, Atmos. Chem. Phys., 4(6), 1461–1738, doi:10.5194/acp-4-1461-2004, 2004.

Atkinson, R., Baulch, D. L., Cox, R. A., Crowley, J. N., Hampson, R. F., Hynes, R. G., Jenkin, M. E., Rossi, M. J., Troe, J.

630   and IUPAC Subcommittee: Evaluated kinetic and photochemical data for atmospheric chemistry: Volume II – gas phase reactions of organic species, Atmos. Chem. Phys., 6(11), 3625–4055, doi:10.5194/acp-6-3625-2006, 2006.

Barber, V. P., Pandit, S., Green, A. M., Trongsiriwat, N., Walsh, P. J., Klippenstein, S. J. and Lester, M. I.: Four-Carbon Criegee Intermediate from Isoprene Ozonolysis: Methyl Vinyl Ketone Oxide Synthesis, Infrared Spectrum, and OH Production, J. Am. Chem. Soc., 140(34), 10866–10880, doi:10.1021/jacs.8b06010, 2018.

635   Bardouki, H., Berresheim, H., Vrekoussis, M., Sciare, J., Kouvarakis, G., Oikonomou, K., Schneider, J. and Mihalopoulos, N.: Gaseous (DMS , MSA , SO_2, H_2SO_4 and DMSO) and particulate (sulfate and methanesulfonate) sulfur species over the northeastern coast of Crete, Atmos. Chem. Phys., 3, 1871–1886, doi:10.5194/acp-3-1871-2003, 2003.

Berland, K., Rose, C., Pey, J., Culot, A., Freney, E., Kalivitis, N., Kouvarakis, G., Cerro, J. C., Mallet, M., Sartelet, K., Beckmann, M., Bourriane, T., Roberts, G., Marchand, N., Mihalopoulos, N. and Sellegri, K.: Spatial extent of new

640   particle formation events over the Mediterranean Basin from multiple ground-based and airborne measurements, Atmos. Chem. Phys., 17, 9567–9583, doi:10.5194/acp-17-9567-2017, 2017.

Berndt, T., Voigtländer, J., Stratmann, F., Junninen, H., Mauldin, R. L., Sipilä, M., Kulmala, M. and Herrmann, H.: Competing atmospheric reactions of CH_2OO with SO_2 and water vapour, Phys. Chem. Chem. Phys., 16(36), 19130, doi:10.1039/C4CP02345E, 2014a.

645   Berndt, T., Jokinen, T., Sipila, M., Mauldin, R. L., Herrmann, H., Stratmann, F., Junninen, H. and Kulmala, M.: H_2SO_4 formation from the gas-phase reaction of stabilized Criegee Intermediates with SO_2: Influence of water vapour content and temperature, Atmos. Environ., 89, 603–612, doi:10.1016/j.atmosenv.2014.02.062, 2014b.

Berresheim, H., Elste, T., Plass-Dülmer, C., Eisele, F. L. and Tanner, D. J.: Chemical ionization mass spectrometer for long-term measurements of atmospheric OH and H_2SO_4, Int. J. Mass Spectrom., 202, 91–109, doi:10.1016/S1387-

650   3806(00)00233-5, 2000.

Berresheim, H., Elste, T., Tremmel, H. G., Allen, A. G., Hansson, H., Rosman, K., Maso, M. D., Mäkelä, J. M., Kulmala, M. and O'Dowd, C. D.: Gas-aerosol relationships of H_2SO_4, MSA , and OH : Observations in the coastal marine boundary layer at Mace Head , Ireland, J. Geophys. Res., 107, 1–12, doi:10.1029/2000JD000229, 2002.

Berresheim, H., Plass-Dülmer, C., Elste, T., Mihalopoulos, N. and Rohrer, F.: OH in the coastal boundary layer of Crete

655   during MINOS: Measurements and relationship with ozone photolysis, Atmos. Chem. Phys., 3(3), 639–649, 2003.

Berresheim, H., Adam, M., Monahan, C., O'Dowd, C., Plane, J. M. C., Bohn, B. and Rohrer, F.: Missing SO_2 oxidant in the coastal atmosphere? - Observations from high-resolution measurements of OH and atmospheric sulfur compounds,

Atmos. Chem. Phys., 14(22), 12209–12223, doi:10.5194/acp-14-12209-2014, 2014.

Birmili, W., Wiedensohler, A., Plass-Dülmer, C. and Berresheim, H.: Evolution of Newly Formed Aerosol Particles in the
660   Continental Boundary Layer : A Case Study Including OH and H_2SO_4 Measurements, Geophys. Res. Lett., 27(15), 2205–
       2208, 2000.

Blitz, M. A., Salter, R. J., Heard, D. E. and Seakins, P. W.: An Experimental and Master Equation Study of the Kinetics of
       OH/OD + SO_2 : The Limiting High-Pressure Rate Coefficients, J. Phys. Chem. A, 121(17), 3184–3191,
       doi:10.1021/acs.jpca.7b01295, 2017a.

665 Blitz, M. A., Salter, R. J., Heard, D. E. and Seakins, P. W.: An Experimental Study of the Kinetics of OH/OD(v = 1,2,3) +
       SO_2 : The Limiting High-Pressure Rate Coefficients as a Function of Temperature, J. Phys. Chem. A, 121(17), 3175–
       3183, doi:10.1021/acs.jpca.7b01294, 2017b.

Boy, M., Kulmala, M., Ruuskanen, T. M., Pihlatie, M., Reissell, A., Aalto, P. P., Keronen, P., Dal Maso, M., Hellen, H.,
       Hakola, H., Jansson, R., Hanke, M. and Arnold, F.: Sulphuric acid closure and contribution to nucleation mode particle
670   growth, Atmos. Chem. Phys., 5(4), 863–878, doi:10.5194/acp-5-863-2005, 2005.

Boy, M., Mogensen, D., Smolander, S., Zhou, L., Nieminen, T., Paasonen, P., Plass-Dülmer, C., Sipilä, M., Petäjä, T.,
       Mauldin, L., Berresheim, H. and Kulmala, M.: Oxidation of SO_2 by stabilized Criegee intermediate (sCI) radicals as a
       crucial source for atmospheric sulfuric acid concentrations, Atmos. Chem. Phys., 13(7), 3865–3879, doi:10.5194/acp-13-
       3865-2013, 2013.

675 Burkholder, J. B., Sander, S. P., Abbat, J., Barker, J. R., Huie, R. E., Kolb, C. E., Kurylo, M. J., Orkin, V. L., Wilmouth, D.
       M. and Wine, P. H.: Chemical Kinetics and Photochemical Data for Use in Atmospheric Studies, Evaluation No. 18, JPL
       Publication 15-10, Jet Propulsion Laboratory, Pasadena, [online] Available from: http://jpldataeval.jpl.nasa.gov/, 2015.

Burkholder, J. B., Sander, S. P., Abbatt, J., Barker, J. R., Cappa, C., Crounse, J. D., Dibble, T. S., Huie, R. E., Kolb, C. E.,
       Kurylo, M. J., Orkin, V. L., Percival, C. J., Wilmouth, D. M. and Wine, P. H.: Chemical Kinetics and Photochemical
680   Data for Use in Atmospheric Studies, Evaluation No. 19, JPL Publication 19-5, Jet Propulsion Laboratory, Pasadena,
       [online] Available from: http://jpldataeval.jpl.nasa.gov/, 2019.

Calvert, J. G. and Stockwell, W. R.: Acid generation in the troposphere by gas-phase chemistry, Environ. Sci. Technol.,
       17(9), 428A–43A, doi:10.1021/es00115a727, 1983.

Caravan, R. L., Vansco, M. F., Au, K., Khan, M. A. H., Li, Y.-L., Winiberg, F. A. F., Zuraski, K., Lin, Y.-H., Chao, W.,
685   Trongsiriwat, N., Walsh, P. J., Osborn, D. L., Percival, C. J., Lin, J. J.-M., Shallcross, D. E., Sheps, L., Klippenstein, S.
       J., Taatjes, C. A. and Lester, M. I.: Direct kinetic measurements and theoretical predictions of an isoprene-derived
       Criegee intermediate, Proc. Natl. Acad. Sci., 117(18), 9733–9740, doi:10.1073/pnas.1916711117, 2020.

Chao, W., Hsieh, J.-T., Chang, C.-H. and Lin, J. J.-M.: Direct kinetic measurement of the reaction of the simplest Criegee
       intermediate with water vapor, Science (80-.)., 347(6223), 751–754, doi:10.1126/science.1261549, 2015.

690 Chhantyal-Pun, R., Welz, O., Savee, J. D., Eskola, A. J., Lee, E. P. F., Blacker, L., Hill, H. R., Ashcroft, M., Khan, M. A. H.,
       Lloyd-Jones, G. C., Evans, L., Rotavera, B., Huang, H., Osborn, D. L., Mok, D. K. W., Dyke, J. M., Shallcross, D. E.,

Percival, C. J., Orr-Ewing, A. J. and Taatjes, C. A.: Direct Measurements of Unimolecular and Bimolecular Reaction Kinetics of the Criegee Intermediate $(CH_3)_2COO$, J. Phys. Chem. A, 121(1), 4–15, doi:10.1021/acs.jpca.6b07810, 2017.

695 Chhantyal-Pun, R., Khan, M. A. H., Martin, R., Zachhuber, N., Buras, Z. J., Percival, C. J., Shallcross, D. E. and Orr-Ewing, A. J.: Direct Kinetic and Atmospheric Modeling Studies of Criegee Intermediate Reactions with Acetone, ACS Earth Sp. Chem., 3, 2363–2371, doi:10.1021/acsearthspacechem.9b00213, 2019.

Cox, R. A. and Penkett, S. A.: Oxidation of Atmospheric SO_2 by Products of the Ozone-Olefin Reaction, Nature, 230, 321–322, 1971.

Criegee, R.: Mechanism of Ozonolysis, Angew. Chem. Int. Ed. Engl., 14(11), 745–752, 1975.

700 Criegee, R. and Wenner, G.: Die Ozonisierung des 9,10-Oktalins, Justus Liebigs Ann. Chem., 564(1), 9–15, doi:10.1002/jlac.19495640103, 1949.

Debevec, C., Sauvage, S., Gros, V., Salameh, T., Sciare, J., Dulac, F. and Locoge, N.: Seasonal variation and origins of volatile organic compounds observed during 2 years at a western Mediterranean remote background site (Ersa , Cape Corsica), Atmos. Chem. Phys., 21, 1449–1484, doi:10.5194/acp-21-1449-2021, 2021.

705 Donahue, N. M., Drozd, G. T., Epstein, S. A., Presto, A. A. and Kroll, J. H.: Adventures in ozoneland: down the rabbit-hole, Phys. Chem. Chem. Phys., 13(23), 10848, doi:10.1039/c0cp02564j, 2011.

Dulac, F., Hamonou, E., Sauvage, S. and Debevec, C.: Introduction to the volume 1 of Atmospheric Chemistry in the Mediterranean and to the ChArMEx experimental effort, in Atmospheric Chemistry in the Mediterranean - Vol. 1, Background Information and Pollutants Distribution, Springer, in press., 2021.

710 Dunne, E. M., Gordon, H., Kürten, A., Almeida, J., Duplissy, J., Williamson, C., Ortega, I. K., Pringle, K. J., Adamov, A., Baltensperger, U., Barmet, P., Benduhn, F., Bianchi, F., Breitenlechner, M., Clarke, A., Curtius, J., Dommen, J., Donahue, N. M., Ehrhart, S., Flagan, R. C., Franchin, A., Guida, R., Hakala, J., Hansel, A., Heinritzi, M., Jokinen, T., Kangasluoma, J., Kirkby, J., Kulmala, M., Kupc, A., Lawler, M. J., Lehtipalo, K., Makhmutov, V., Mann, G., Mathot, S., Merikanto, J., Miettinen, P., Nenes, A., Onnela, A., Rap, A., Reddington, C. L. S., Riccobono, F., Richards, N. A. D.,

715 Rissanen, M. P., Rondo, L., Sarnela, N., Schobesberger, S., Sengupta, K., Simon, M., Sipilä, M., Smith, J. N., Stozhkov, Y., Tomé, A., Tröstl, J., Wagner, P. E., Wimmer, D., Winkler, P. M., Worsnop, D. R. and Carslaw, K. S.: Global atmospheric particle formation from CERN CLOUD measurements, Science, 354(6316), 1119–1124, 2016.

Eisele, F. L. and Tanner, D. J.: Ion-Assisted Tropospheric OH Measurements, J. Geophys. Res., 96(D5), 9295–9308, 1991.

Eisele, F. L. and Tanner, D. J.: Measurement of the gas phase concentration of H_2SO_4 and methane sulfonic acid and

720 estimetes of H_2SO_4 production and loss in the atmosphere, J. Geophys. Res., 98, 9001–9010, 1993.

Faloona, I. C., Tan, D., Lesher, R. L., Hazen, N. L., Frame, C. L., Simpas, J. B., Harder, H., Martinez, M., Di Carlo, P., Ren, X. and Brune, W. H.: A Laser-induced Fluorescence Instrument for Detecting Tropospheric OH and HO2 : Characteristics and Calibration, J. Atmos. Chem., 47, 139–167, doi:10.1023/B:JOCH.0000021036.53185.0e, 2004.

Fang, Y., Barber, V. P., Klippenstein, S. J., McCoy, A. B. and Lester, M. I.: Tunneling effects in the unimolecular decay of

725 $(CH_3)_2COO$ Criegee intermediates to OH radical products, J. Chem. Phys., 146(13), 134307, doi:10.1063/1.4979297,

2017.

Finlayson-Pitts, B. J. and Pitts Jr, J. N.: Chemistry of the Upper and Lower Atmosphere: Theory, Experiments, and Applications, Academic Press, San Diego., 2000.

Geron, C., Rasmussen, R., Arnts, R. R. and Guenther, A.: A review and synthesis of monoterpene speciation from forests in the United States, Atmos. Environ., 34, 1761–1781, doi:10.1016/S1352-2310(99)00364-7, 2000.

Hanson, D. R.: Mass Accommodation of H_2SO_4 and CH_3SO_3H on Water - Sulfuric Acid Solutions from 6% to 97% RH, J. Phys. Chem. A, (109), 6919–6927, 2005.

Hanson, D. R. and Eisele, F.: Diffusion of H_2SO_4 in Humidified Nitrogen: Hydrated H_2SO_4, J. Phys. Chem. A, 104(8), 1715–1719, doi:10.1021/jp993622j, 2000.

Hatakeyama, S., Kobayashi, H., Lin, Z. Y., Takagi, H. and Akimoto, H.: Mechanism for the reaction of peroxymethylene with sulfur dioxide, J. Phys. Chem., 90(17), 4131–4135, doi:10.1021/j100408a059, 1986.

Hoefs, J.: Stable isotope geochemistry, Eighth Edition, Springer., 2018.

Huang, H.-L., Chao, W. and Lin, J. J.-M.: Kinetics of a Criegee intermediate that would survive high humidity and may oxidize atmospheric SO_2, Proc. Natl. Acad. Sci., 112(35), 10857–10862, doi:10.1073/pnas.1513149112, 2015.

IUPAC: Task Group on Atmospheric Chemical Kinetic Data Evaluation, http://iupac.pole-ether.fr, last access: April, 2020.

Jefferson, A., Eisele, F. L., Ziemann, P. J., Weber, R. J., Marti, J. J. and Mcmurry, P. H.: Measurements of the H_2SO_4 mass accommodation coefficient onto polydisperse aerosol, J. Geophys. Res. Atmos., 102(D15), 19021–19028, 1997.

Jefferson, A., Tanner, D. J., Eisele, F. L. and Berresheim, H.: Sources and sinks of H_2SO_4 in the remote Antarctic marine boundary layer, J. Geophys. Res. Atmos., 103(D1), 1639–1645, doi:10.1029/97JD01212, 1998.

Johnson, D. and Marston, G.: The gas-phase ozonolysis of unsaturated volatile organic compounds in the troposphere, Chem. Soc. Rev., 37(4), 699–716, doi:10.1039/b704260b, 2008.

Kerminen, V.-M. and Kulmala, M.: Analytical formulae connecting the "real" and the "apparent" nucleation rate and the nuclei number concentration for atmospheric nucleation events, J. Aerosol Sci., 33, 609–622, 2002.

Kesselmeier, J. and Staudt, M.: Biogenic Volatile Organic Compounds (VOC): An Overview on Emission , Physiology and Ecology, J. Atmos. Chem., 33, 23–88, 1999.

Khan, M. A. H., Percival, C. J., Caravan, R. L., Taatjes, C. A. and Shallcross, D. E.: Criegee intermediates and their impacts on the troposphere, Environ. Sci. Process. Impacts, 20(3), 437–453, doi:10.1039/C7EM00585G, 2018.

Kim, S., Guenther, A., Lefer, B., Flynn, J., Griffin, R., Rutter, A. P., Gong, L. and Cevik, B. K.: Potential role of stabilized Criegee radicals in sulfuric acid production in a high biogenic VOC environment, Environ. Sci. Technol., 49(6), 3383–3391, doi:10.1021/es505793t, 2015.

Kuang, C., Mcmurry, P. H., Mccormick, A. V and Eisele, F. L.: Dependence of nucleation rates on sulfuric acid vapor concentration in diverse atmospheric locations, J. Geophys. Res., 113(D10209), 1–9, doi:10.1029/2007JD009253, 2008.

Kukui, A., Ancellet, G. and Le Bras, G.: Chemical ionisation mass spectrometer for measurements of OH and Peroxy radical concentrations in moderately polluted atmospheres, J. Atmos. Chem., 61(2), 133–154, doi:10.1007/s10874-009-9130-9,

760   2008.

Kukui, A., Legrand, M., Ancellet, G., Gros, V., Bekki, S., Loisil, R. and Preunkert, S.: Measurements of OH and RO_2 radicals at the coastal Antarctic site of Dumont d ' Urville (East Antarctica) in summer 2010 – 2011, J. Geophys. Res., 117, D12310, doi:10.1029/2012JD017614, 2012.

Kukui, A., Legrand, M., Preunkert, S., Frey, M. M., Loisil, R., Roca, J. G., Jourdain, B., King, M. D. and Pierre, U.:

765   Measurements of OH and RO_2 radicals at Dome C , East Antarctica, Atmos. Chem. Phys., 14, 12373–12392, doi:10.5194/acp-14-12373-2014, 2014.

Kulmala, M., Petäjä, T., Nieminen, T., Sipilä, M., Manninen, H. E., Lehtipalo, K., Dal Maso, M., Aalto, P. P., Junninen, H., Paasonen, P., Riipinen, I., Lehtinen, K. E. J., Laaksonen, A. and Kerminen, V.-M.: Measurement of the nucleation of atmospheric aerosol particles, Nat. Protoc., 7(9), 1651–1667, doi:10.1038/nprot.2012.091, 2012.

770   Kürten, A., Jokinen, T., Simon, M., Sipilä, M., Sarnela, N., Junninen, H., Adamov, A., Almeida, J., Amorim, A., Bianchi, F., Breitenlechner, M., Dommen, J., Donahue, N. M., Duplissy, J., Ehrhart, S., Flagan, R. C., Franchin, A., Hakala, J., Hansel, A., Heinritzi, M., Hutterli, M., Kangasluoma, J., Kirkby, J., Laaksonen, A., Lehtipalo, K., Leiminger, M., Makhmutov, V., Mathot, S., Onnela, A., Petäjä, T., Praplan, A. P., Riccobono, F., Rissanen, M. P., Rondo, L., Schobesberger, S., Seinfeld, J. H., Steiner, G., Tomé, A., Tröstl, J., Winkler, P. M., Williamson, C., Wimmer, D., Ye, P.,

775   Baltensperger, U., Carslaw, K. S., Kulmala, M., Worsnop, D. R. and Curtius, J.: Neutral molecular cluster formation of sulfuric acid – dimethylamine observed in real time under atmospheric conditions, Proc. Natl. Acad. Sci., 111(42), 15019–15024, doi:10.1073/pnas.1404853111, 2014.

Kürten, A., Bergen, A., Heinritzi, M., Leiminger, M., Lorenz, V., Piel, F., Simon, M., Sitals, R., Wagner, A. C. and Curtius, J.: Observation of new particle formation and measurement of sulfuric acid , ammonia , amines and highly oxidized

780   organic molecules at a rural site in central Germany, Atmos. Chem. Phys., 16, 12793–12813, doi:10.5194/acp-16-12793-2016, 2016.

Kürten, A., Li, C., Bianchi, F., Curtius, J., Dias, A., Donahue, N. M., Duplissy, J., Flagan, R. C., Hakala, J., Jokinen, T., Kirkby, J., Kulmala, M., Laaksonen, A., Lehtipalo, K., Makhmutov, V., Onnela, A., Rissanen, M. P., Simon, M., Sipilä, M., Stozhkov, Y., Tröstl, J., Ye, P. and McMurry, P. H.: New particle formation in the sulfuric acid – dimethylamine –

785   water system : reevaluation of CLOUD chamber measurements and comparison to an aerosol nucleation and growth model, Atmos. Chem. Phys., 18, 845–863, 2018.

Kurtén, T., Lane, J. R., Jørgensen, S. and Kjaergaard, H. G.: A Computational Study of the Oxidation of SO_2 to SO_3 by Gas-Phase Organic Oxidants, J. Phys. Chem. A, 115(31), 8669–8681, doi:10.1021/jp203907d, 2011.

Kuwata, K. T., Guinn, E. J., Hermes, M. R., Fernandez, J. A., Mathison, J. M. and Huang, K.: A Computational Re-

790   examination of the Criegee Intermediate-Sulfur Dioxide Reaction, J. Phys. Chem. A, 119(41), 10316–10335, doi:10.1021/acs.jpca.5b06565, 2015.

Lester, M. I. and Klippenstein, S. J.: Unimolecular Decay of Criegee Intermediates to OH Radical Products: Prompt and Thermal Decay Processes, Acc. Chem. Res., 51, 978–985, doi:10.1021/acs.accounts.8b00077, 2018.

Lewis, T. R., Blitz, M. A., Heard, D. E. and Seakins, P. W.: Direct evidence for a substantive reaction between the Criegee
795   intermediate, CH2OO, and the water vapour dimer, Phys. Chem. Chem. Phys., 17(7), 4859–4863,
        doi:10.1039/C4CP04750H, 2015.

Li, Y.-L., Kuo, M.-T. and Lin, J. J.-M.: Unimolecular decomposition rates of a methylsubstituted Criegee intermediate syn-
        CH3CHOO, RSC Adv., 10, 8518–8524, doi:10.1039/D0RA01406K, 2020.

Lin, L.-C., Chao, W., Chang, C.-H., Takahashi, K. and Lin, J. J.-M.: Temperature dependence of the reaction of anti-
800   CH3CHOO with water vapor, Phys. Chem. Chem. Phys., 18(40), 28189–28197, doi:10.1039/C6CP05171E, 2016.

Lin, Y.-H., Yin, C., Takahashi, K., Lin, J.-M.; Surprisingly long lifetime of methacrolein oxide, an isoprene derived Criegee
        intermediate, under humid conditions, Commun. Chem., 4(12), https://doi.org/10.1038/s42004-021-00451-z, 2021.

Mallik, C., Tomsche, L., Bourtsoukidis, E., Crowley, J. N., Derstroff, B., Fischer, H., Hafermann, S., Hüser, I., Javed, U.,
        Keßel, S., Lelieveld, J., Martinez, M., Meusel, H., Novelli, A., Phillips, G. J., Pozzer, A., Reiffs, A., Sander, R.,
805   Taraborrelli, D., Sauvage, C., Schuladen, J., Su, H., Williams, J. and Harder, H.: Oxidation processes in the eastern
        Mediterranean atmosphere : evidence from the modelling of HOx measurements over Cyprus, Atmos. Chem. Phys.,
        18(14), 10825–10847, 2018.

Mauldin III, R. L., Berndt, T., Sipilä, M., Paasonen, P., Petäjä, T., Kim, S., Kurtén, T., Stratmann, F., Kerminen, V.-M. and
        Kulmala, M.: A new atmospherically relevant oxidant of sulphur dioxide, Nature, 488(7410), 193–196,
810   doi:10.1038/nature11278, 2012.

Medeiros, D. J., Blitz, M. A. and Seakins, P. W.: Exploring the features on the OH + SO2 potential energy surface using
        theory and testing its accuracy by comparison to experimental data, Phys. Chem. Chem. Phys., 20, 8984–8990,
        doi:10.1039/C8CP00091C, 2018.

Michoud, V., Sciare, J., Sauvage, S., Dusanter, S., Léonardis, T., Gros, V., Kalogridis, C., Zannoni, N., Féron, A., Petit, J.-E.
815   E., Crenn, V., Baisnée, D., Sarda-Estève, R., Bonnaire, N., Marchand, N., Dewitt, H. L., Pey, J., Colomb, A., Gheusi, F.,
        Szidat, S., Stavroulas, I., Borbon, A. and Locoge, N.: Organic carbon at a remote site of the western Mediterranean
        Basin : sources and chemistry during the ChArMEx SOP2 field experiment, Atmos. Chem. Phys., 17(14), 8837–8865,
        doi:10.5194/acp-17-8837-2017, 2017.

Newland, M. J., Rickard, A. R., Sherwen, T., Evans, M. J., Vereecken, L., Muñoz, A., Ródenas, M., Bloss, W. J., Newland,
820   C. M. J. and Rickard, A. R.: The atmospheric impacts of monoterpene ozonolysis on global stabilised Criegee
        intermediate budgets and SO2 oxidation : experiment , theory and modelling, Atmos. Chem. Phys., 18, 6095–6120,
        doi:doi.org/10.5194/acp-18-6095-2018, 2018.

Novelli, A., Hens, K., Ernest, C. T., Martinez, M., Nölscher, A. C., Sinha, V., Paasonen, P., Petäjä, T., Sipilä, M., Elste, T.,
        Plass-Dülmer, C., Phillips, G. J., Kubistin, D., Williams, J., Vereecken, L., Lelieveld, J. and Harder, H.: Estimating the
825   atmospheric concentration of Criegee intermediates and their possible interference in a FAGE-LIF instrument, Atmos.
        Chem. Phys., 17(12), 7807–7826, doi:10.5194/acp-17-7807-2017, 2017.

Paasonen, P., Nieminen, T., Asmi, E., Manninen, H. E., Petäjä, T., Plass-Dülmer, C., Flentje, H., Birmili, W., Wiedensohler,

A., Hõrrak, U., Metzger, A., Hamed, A., Laaksonen, A., Facchini, M. C., Kerminen, V.-M. and Kulmala, M.: On the roles of sulphuric acid and low-volatility organic vapours in the initial steps of atmospheric new particle formation, Atmos. Chem. Phys., 10(22), 11223–11242, doi:10.5194/acp-10-11223-2010, 2010.

Petäjä, T., Mauldin III, R. L., Kosciuch, E., McGrath, J., Nieminen, T., Paasonen, P., Boy, M., Adamov, A., Kotiaho, T. and Kulmala, M.: Sulfuric acid and OH concentrations in a boreal forest site, Atmos. Chem. Phys., 9, 7435–7448, 2009.

Pöschl, U., Canagaratna, M., Jayne, J. T., Molina, L. T., Worsnop, D. R., Kolb, C. E. and Molina, M. J.: Mass Accommodation Coefficient of H_2SO_4 Vapor on Aqueous Sulfuric Acid Surfaces and Gaseous Diffusion Coefficient of H_2SO_4 in N_2/H_2O, J. Phys. Chem. A, 102(49), 10082–10089, doi:10.1021/jp982809s, 1998.

Rissler, J., Vestin, A., Swietlicki, E., Fisch, G., Zhou, J., Artaxo, P. and Andreae, M. O.: Size distribution and hygroscopic properties of aerosol particles from dry-season biomass burning in Amazonia, Atmos. Chem. Phys., 6(2), 471–491, doi:10.5194/acp-6-471-2006, 2006.

Ruscic, B.: Active Thermochemical Tables: Water and Water Dimer, J. Phys. Chem. A, 117, 11940−11953, doi:10.1021/jp403197t, 2013.

Seinfeld, J. H. and Pandis, S. N.: Atmospheric chemistry and physics : from air pollution to climate change, John Wiley & Sons, Inc., Hoboken, New Jersey., 2016.

Sheps, L., Scully, A. M. and Au, K.: UV absorption probing of the conformer-dependent reactivity of a Criegee intermediate CH_3CHOO, Phys. Chem. Chem. Phys., 16(48), 26701–26706, doi:10.1039/C4CP04408H, 2014.

Sheps, L., Rotavera, B., Eskola, A. J., Osborn, D. L., Taatjes, C. A., Au, K., Shallcross, D. E., Khan, M. A. H. and Percival, C. J.: The Reaction of Criegee Intermediate CH_2OO with Water Dimer: Primary Products and Atmospheric Impact, Phys. Chem. Chem. Phys., 19(33), 21970–21979, doi:10.1039/C7CP03265J, 2017.

Sihto, S., Kulmala, M., Kerminen, V., Maso, M. D. and Pet, T.: Atmospheric sulphuric acid and aerosol formation : implications from atmospheric measurements for nucleation and early growth mechanisms, Atmos. Chem. Phys., 6, 4079–4091, doi:10.5194/acp-6-4079-2006, 2006.

Sipilä, M., Berndt, T., Petäjä, T., Brus, D., Vanhanen, J., Stratmann, F., Patokoski, J., Mauldin, R. L., Hyvärinen, A.-P., Lihavainen, H. and Kulmala, M.: The Role of Sulfuric Acid in Atmospheric Nucleation, Science (80-.)., 327(5970), 1243 LP – 1246, doi:10.1126/science.1180315, 2010.

Smith, J. N., Moore, K. F., Eisele, F. L., Voisin, D., Ghimire, A. K., Sakurai, H. and McMurry, P. H.: Chemical composition of atmospheric nanoparticles during nucleation events in Atlanta, J. Geophys. Res., 110(D22), D22S03, doi:10.1029/2005JD005912, 2005.

Smith, M. C., Chang, C. H., Chao, W., Lin, L. C., Takahashi, K., Boering, K. A. and Lin, J. J. M.: Strong negative temperature dependence of the simplest criegee intermediate CH_2OO reaction with water dimer, J. Phys. Chem. Lett., 6(14), 2708–2713, doi:10.1021/acs.jpclett.5b01109, 2015.

Smith, M. C., Chao, W., Takahashi, K., Boering, K. A. and Lin, J. J. M.: Unimolecular Decomposition Rate of the Criegee Intermediate $(CH_3)_2COO$ Measured Directly with UV Absorption Spectroscopy, J. Phys. Chem. A, 120(27), 4789–4798,

doi:10.1021/acs.jpca.5b12124, 2016.

Stolzenburg, D., Fischer, L., Vogel, A. L., Heinritzi, M., Schervish, M., Simon, M., Wagner, A. C., Dada, L., Ahonen, L. R., Amorim, A., Baccarini, A., Bauer, P. S., Baumgartner, B., Bergen, A., Bianchi, F., Breitenlechner, M., Brilke, S., Buenrostro Mazon, S., Chen, D., Dias, A., Draper, D. C., Duplissy, J., El Haddad, I., Finkenzeller, H., Frege, C., Fuchs, C., Garmash, O., Gordon, H., He, X., Helm, J., Hofbauer, V., Hoyle, C. R., Kim, C., Kirkby, J., Kontkanen, J., Kürten, A., Lampilahti, J., Lawler, M., Lehtipalo, K., Leiminger, M., Mai, H., Mathot, S., Mentler, B., Molteni, U., Nie, W., Nieminen, T., Nowak, J. B., Ojdanic, A., Onnela, A., Passananti, M., Petäjä, T., Quéléver, L. L. J., Rissanen, M. P., Sarnela, N., Schallhart, S., Tauber, C., Tomé, A., Wagner, R., Wang, M., Weitz, L., Wimmer, D., Xiao, M., Yan, C., Ye, P., Zha, Q., Baltensperger, U., Curtius, J., Dommen, J., Flagan, R. C., Kulmala, M., Smith, J. N., Worsnop, D. R., Hansel, A., Donahue, N. M. and Winkler, P. M.: Rapid growth of organic aerosol nanoparticles over a wide tropospheric temperature range, Proc. Natl. Acad. Sci., 115(37), 9122–9127, doi:10.1073/pnas.1807604115, 2018.

Stone, D., Blitz, M., Daubney, L., Howes, N. U. M. and Seakins, P.: Kinetics of CH_2OO reactions with SO_2, NO_2, NO, H_2O and CH_3CHO as a function of pressure, Phys. Chem. Chem. Phys., 16(3), 1139–1149, doi:10.1039/C3CP54391A, 2014.

Stone, D., Au, K., Sime, S., Medeiros, D. J., Blitz, M., Seakins, P. W. and Sheps, L.: Unimolecular decomposition kinetics of the stabilised Criegee intermediates CH_2OO and, Phys. Chem. Chem. Phys., (20), 24940–24954, doi:10.1039/C8CP05332D, 2018.

Taatjes, C. A., Welz, O., Eskola, A. J., Savee, J. D., Scheer, A. M., Shallcross, D. E., Rotavera, B., Lee, E. P. F., Dyke, J. M., Mok, D. K. W., Osborn, D. L. and Percival, C. J.: Direct Measurements of Conformer-Dependent Reactivity of the Criegee Intermediate CH_3CHOO, Science (80-.)., 340(6129), 177–180, doi:10.1126/science.1234689, 2013.

Tröstl, J., Chuang, W. K., Gordon, H., Heinritzi, M., Yan, C., Molteni, U., Ahlm, L., Frege, C., Bianchi, F., Wagner, R., Simon, M., Lehtipalo, K., Williamson, C., Craven, J. S., Duplissy, J., Adamov, A., Almeida, J., Bernhammer, A., Breitenlechner, M., Gysel, M., Hansel, A., Hoyle, C. R., Jokinen, T., Junninen, H., Kangasluoma, J., Sipilä, M., Smith, J. N., Steiner, G., Tomè, A., Virtanen, A., Wagner, A. C., Dommen, J., Kirkby, J., Kulmala, M., Riipinen, I., Worsnop, D. R., Donahue, N. M. and Baltensperger, U.: The role of low-volatility organic compounds in initial particle growth in the atmosphere, Nature, 533, 527, doi:10.1038/nature18271, 2016.

Vereecken, L. and Francisco, J. S.: Theoretical studies of atmospheric reaction mechanisms in the troposphere, Chem. Soc. Rev., 41(19), 6259, doi:10.1039/c2cs35070j, 2012.

Vereecken, L., Harder, H. and Novelli, A.: The reaction of Criegee intermediates with NO, RO2, and SO2, and their fate in the atmosphere, Phys. Chem. Chem. Phys., 14(42), 14682, doi:10.1039/c2cp42300f, 2012.

Vereecken, L., Novelli, A. and Taraborrelli, D.: Unimolecular decay strongly limits the atmospheric impact of Criegee intermediates, Phys. Chem. Chem. Phys., 19, 31599–31612, doi:10.1039/C7CP05541B, 2017.

Villani, P., Picard, D., Michaud, V., Laj, P. and Wiedensohler, A.: Design and Validation of a Volatility Hygroscopic Tandem Differential Mobility Analyzer (VH-TDMA) to Characterize the Relationships Between the Thermal and Hygroscopic Properties of Atmospheric Aerosol Particles, Aerosol Sci. Technol., 42(9), 729–741,

doi:10.1080/02786820802255668, 2008.

Wang, Y.-Y., Dash, M. R., Chung, C.-Y. and Lee, Y.-P.: Detection of transient infrared absorption of SO_3 and 1,3,2-dioxathietane-2,2-dioxide [cyc-$(CH_2)O(SO_2)O$] in the reaction CH_2OO+SO_2, J. Chem. Phys., 148(6), 064301, doi:10.1063/1.5019205, 2018.

Weber, R. J., Marti, J. J., Mcmurry, P. H., Eisele, F. L., Tanner, D. J. and Jefferson, A.: Measurements of new particle formation and ultrafine particle growth rates at a clean continental site, J. Geophys. Res., 102, 4375–4385, 1997.

Welz, O., Savee, J. D., Osborn, D. L., Vasu, S. S., Percival, C. J., Shallcross, D. E. and Taatjes, C. A.: Direct Kinetic Measurements of Criegee Intermediate (CH_2OO) Formed by Reaction of CH2I with O_2, Science, 335(6065), 204–207, doi:10.1126/science.1213229, 2012.

Yao, L., Garmash, O., Bianchi, F., Zheng, J., Yan, C., Paasonen, P., Sipilä, M., Wang, M., Wang, X. and Xiao, S.: Atmospheric new particle formation from sulfuric acid and amines in a Chinese megacity, Science, 361(6399), 278–281, doi:10.1126/science.aao4839 , 2018.

Yao, L., Fan, X., Yan, C., Kurtén, T., Daellenbach, K. R., Li, C., Wang, Y., Guo, Y., Dada, L., Rissanen, M. P., Cai, J., Tham, Y. J., Zha, Q., Zhang, S., Du, W., Yu, M., Zheng, F., Zhou, Y., Kontkanen, J., Chan, T., Shen, J., Kujansuu, J. T., Kangasluoma, J., Jiang, J., Wang, L., Worsnop, D. R., Petäjä, T., Kerminen, V.-M., Liu, Y., Chu, B., He, H., Kulmala, M. and Bianchi, F.: Unprecedented Ambient Sulfur Trioxide (SO_3) Detection: Possible Formation Mechanism and Atmospheric Implications, Environ. Sci. Technol. Lett., doi:10.1021/acs.estlett.0c00615, 2020.

York, D., Evensen, N. M., Martínez, M. L. and De Basabe Delgado, J.: Unified equations for the slope, intercept, and standard errors of the best straight line, Am. J. Phys., 72(3), 367–375, doi:10.1119/1.1632486, 2004.

Zannoni, N., Dusanter, S., Gros, V., Sarda Esteve, R., Michoud, V., Sinha, V., Locoge, N. and Bonsang, B.: Intercomparison of two comparative reactivity method instruments inf the Mediterranean basin during summer 2013, Atmos. Meas. Tech., 8(9), 3851–3865, doi:10.5194/amt-8-3851-2015, 2015.

Zannoni, N., Gros, V., Sarda Esteve, R., Kalogridis, C., Michoud, V., Dusanter, S., Sauvage, S., Locoge, N., Colomb, A. and Bonsang, B.: Summertime OH reactivity from a receptor coastal site in the Mediterranean Basin, Atmos. Chem. Phys., 17(20), 12645–12658, doi:10.5194/acp-17-12645-2017, 2017.

Zhang, R., Khalizov, A., Wang, L., Hu, M., and Xu, W.: Nucleation and Growth of Nanoparticles in the Atmosphere, Chem. Rev., 112, 1957-2011, doi:10.1021/cr2001756, 2012.